FINAL REPORT

The Relationship Between Permeability Coefficients for Soil Obtained Using Liquid and Gas

Richard P. Long, Professor
Kenneth R. Demars, Associate Professor
Raafat R. Mankbadi, Graduate Student
Alvaro Covo, Graduate Student

September 1988

JHR 88-180 Project 86-5

This research was sponsored by the Joint Highway Research Advisory Council of the University of Connecticut and the Connecticut Department of Transportation and was carried out in the Civil Engineering Department of The University of Connecticut.

FINAL REPORT

The Relationship Between Permeability Coefficients for Soil Obtained Using Liquid and Gas

by

Richard P. Long, Professor
Kenneth R. Demars, Associate Professor
Raafat R. Mankbadi, Graduate Student
Alvaro Covo, Graduate Student

This research was sponsored by the Joint Highway Research Advisory Council of the University of Connecticut and the Connecticut Department of Transportation and was carried out in the Civil Engineering Department of the University of Connecticut.

TABLE OF CONTENTS

Introduction

The permeability of porous media to gases and liquids has attracted a considerable amount of attention over the past several decades. Interest in such studies has been motivated by several possible applications. Diverse fields as soil mechanics, petroleum engineering, ground water hydrology, environmental engineering, and gas separations require understanding of such flow phenomena. The importance of the permeability coefficient of foundation materials beneath a highway pavement is well known. Soils with high permeability coefficients are usually associated with good pavement foundations. Low permeability soils are often subject to pumping and frost heave.

Water is the most common permeant of interest in soils, but the relation between water and gas flow indicates that permeability can be measured using either fluid. Little work has been done to date on determining this property of soils.

Previous work on permeability to air has shown that for granular soil a reasonably accurate permeability to water can be predicted from the results (Klinkenberg 1941). Measuring the permeability using water requires certain precautions since any air dissolved in the water tends to come out of solution and block some of the porous passages within the soil yielding a value of the coefficient of permeability from the experimental results that is too low.

In this report an alternative way of determining soil permeability is presented. The new technique involves measuring the air permeability and then converting it to hydraulic permeability. This procedure works well for granular soils.

Background

Theory of Gas Movement in Porous Media

As a gas flows in a capillary tube, its progress will be impeded by collisions with other gas molecules and with the capillary walls. Figure (1) (Moore 1975) delineates mechanisms involving only collisions with the walls (Knudsen diffusion), only collisions with other gas molecules (molecular diffusion), both wall and intermolecular collisions (transition region diffusion), hopping or sliding along the capillary wall (surface flow), and finally flow involving all mechanisms (general flow). The type of flow which is likely to predominate depends upon the relative magnitudes of the capillary radius, r, and the mean free path of the molecule (Moore 1975).

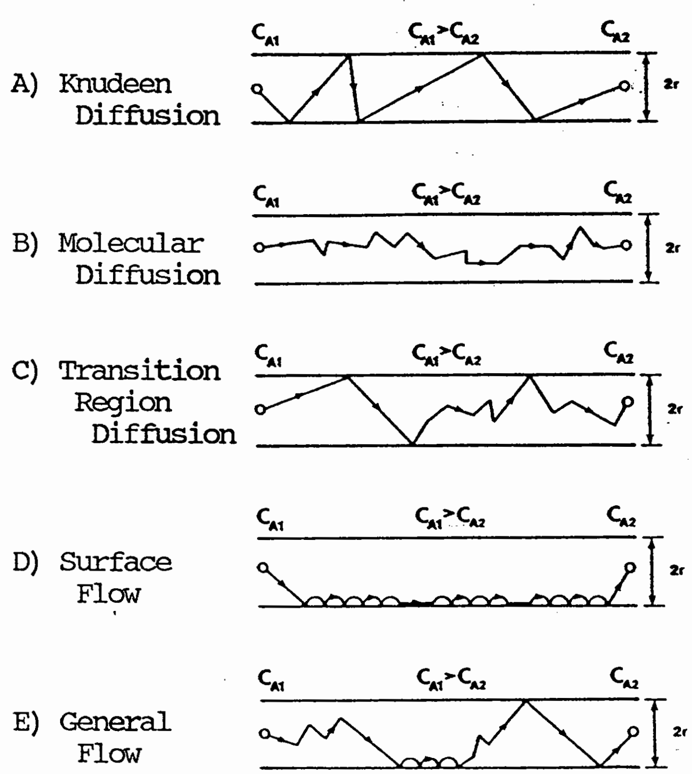

Flow mechanisms for a single gas in a capillary tube.

Figure 1

Pressure Flow in a Capillary Tube

If a total pressure gradient exists in a capillary tube, transport will occur in the direction of decreasing pressure by Poiseuille flow and by slip flow along the capillary walls.

Generalization to Porous Media

Gas flow through porous media is illustrated in Fig. 2. The flow occurs in the tortuous void channels. The only area available for flow correlates with the porosity ($n = V_v/V_t$).

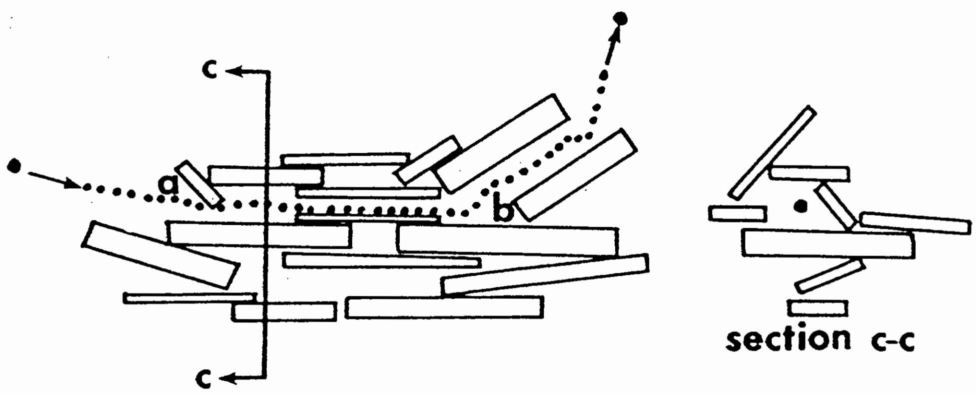

Gas flow path through a porous medium.

Figure 2

Because the predominating flow mechanism is related to the radius of a capillary tube, special consideration must be taken of the wide range of pore sizes encountered when approximating the pores of a soil as a bundle of parallel capillary tubes.

Assuming the soil is homogeneous, the laminar gas movement in the soil may be expressed by Darcy's law as:

$$v = k \text{ grad } P$$

where v = linear flow velocity, k = the permeability coefficient, P = the flow pressure, and "grad" = the vector gradient operator. Actually, in the case of gases the fluid does not stick to the walls of the pores as liquid does and a phenomenon termed "slip" occurs, i.e., the layer of gas next to the surface is in motion with respect to the solid surface. This slip of the fluid along the pore walls gives rise to an apparent dependence of permeability on pressure. An explanation of the flow of gases requires the concept of "slip". This theory was first considered in the literature as long ago as 1875 by Kundt and Warburg, and comprehensively demonstrated by Klinkenberg in 1941. After intensive investigations, using dry Jena Glass filter and core samples with different types of gases and liquid under large range of pressure, Klinkenberg found that:

1. The permeability coefficient as determined with gases is dependent upon the nature of gas, and is approximately a linear function of the reciprocal mean pressure.
2. Gas permeability does not depend on the pressure differences as long as the mean pressure is constant.
3. When the mean free paths are small, e.g., at high pressures, the permeability to gas should be expected to approach as that for liquids. Gas and liquid permeability should therefore be identical if the gas pressure is infinite.

Fig. (3) and (4) show some of Klinkenberg results. As can be seen from the graphs in Fig. 3 a plot of the permeability of porous media against the reciprocal pressure yields a straight line. Extrapolation of the straight line to the vertical axis produces an intercept that indicates the permeability at infinite pressure and should be approximately equal to the hydraulic permeability. Using Klinkenberg theory, it is simple to extrapolate from three measurements of finite mean pressures to the infinite one. Unfortunately Klinkenberg did not investigate his theory on different types of soils. Many interesting questions remain such as:

1. How does the theory of slip apply to particle beds having different packing?
2. Using Klinkenberg theory can we predict the water permeability of the soil from its air permeability? What is the limit of this application?

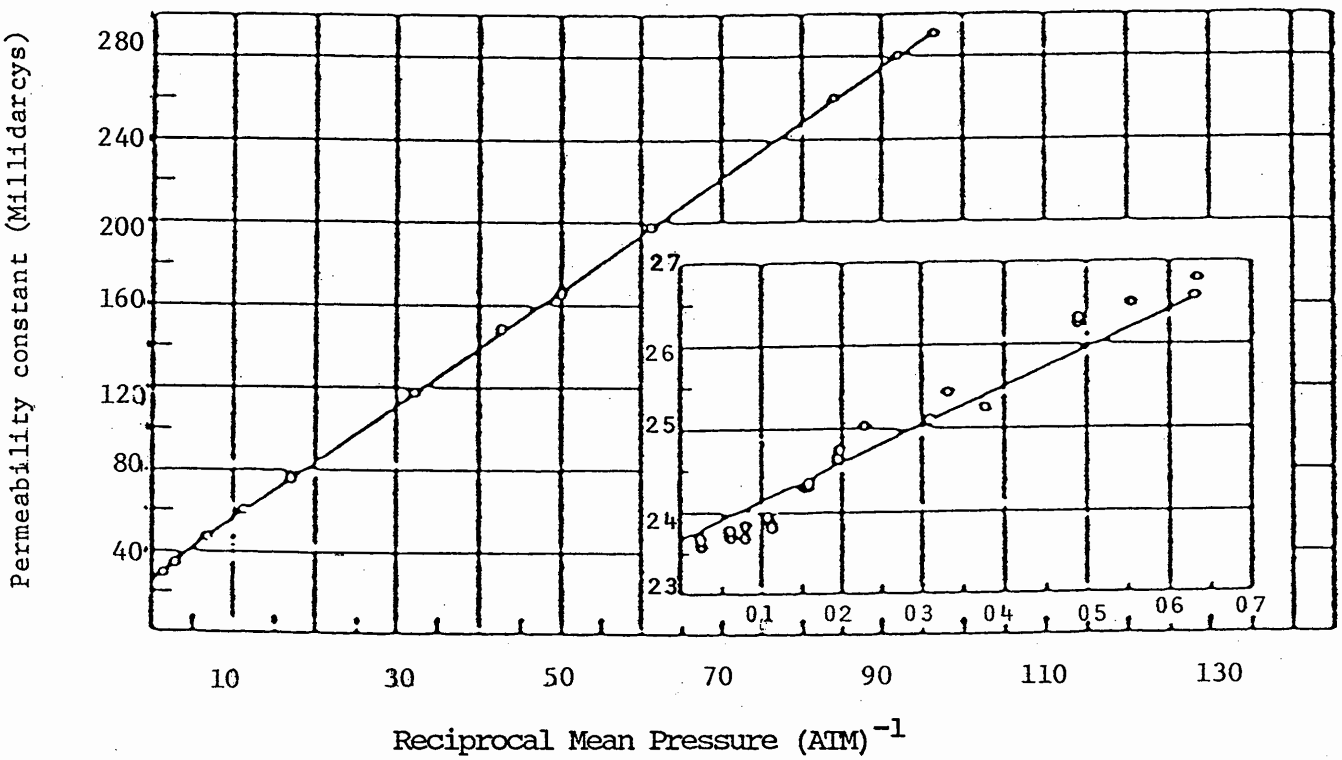

Permeability Constant of Core Sample "A"

to Air at Different Pressures (Permeability

Constant to Isoocatane, 2.36Md)

Figure 3

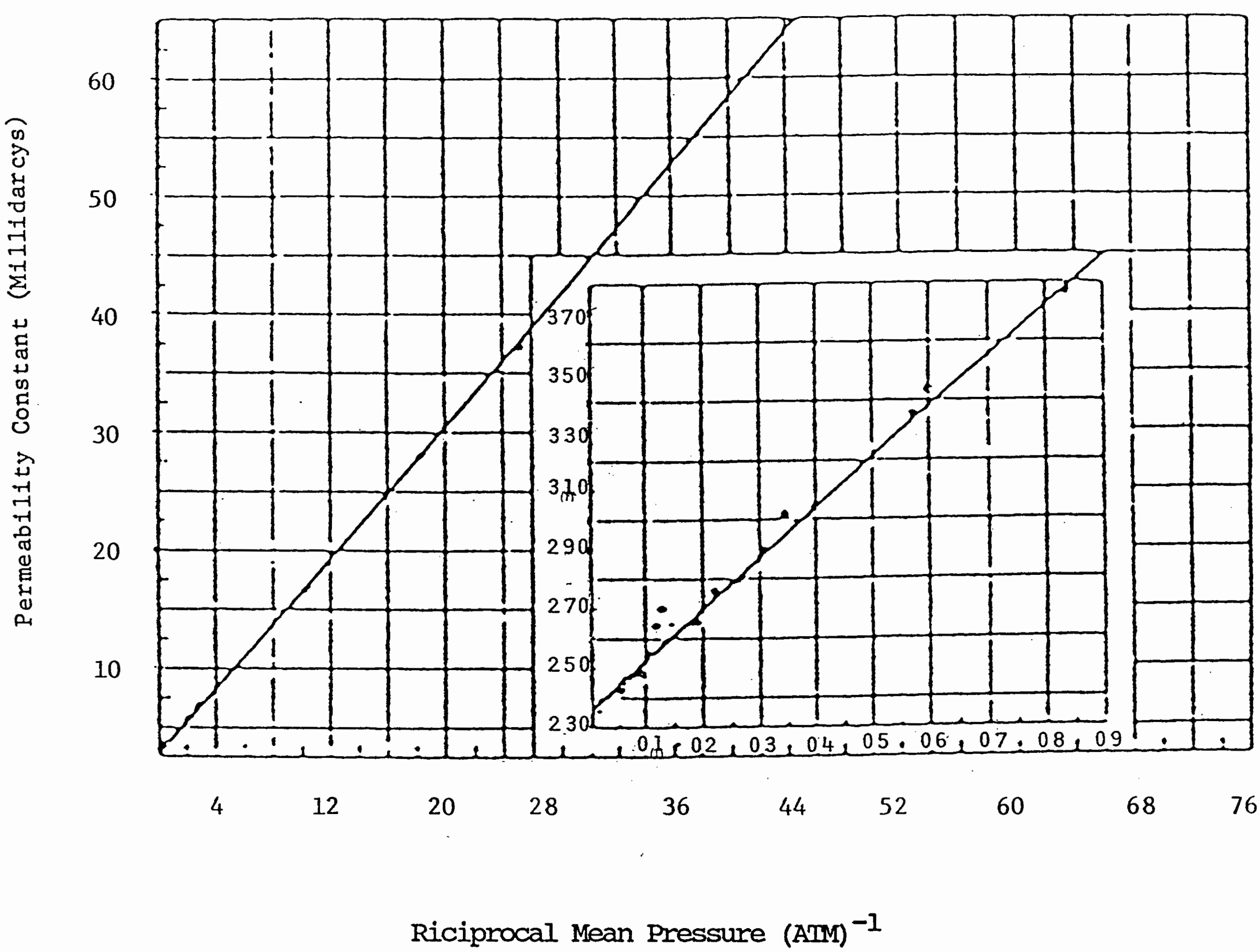

Permeability constant of Jend Glass Filter "GA" to air at different pressures (Permeability constant to Isooctane, 2.36 Md)

Figure 4

3. What is the effect of the structure, grain size distribution, and the porosity of the soil in its air permeability coefficient?

Experimental studies of air permeability in partially saturated clay had been conducted by Matyas (1967). E.L. Matyas concluded that as the stresses on a specimen are increased, the degree of saturation increases, and consequently the air permeability decreases. Matyas was mainly interested in the variation of air permeability with consolidation pressure and he did not investigate the Klinkenberg effect.

In 1971 G.E. Blight examined the unsteady flow of air through silt-like tailings (saturated and unsaturated samples) but he also did not investigate the relation between water and air permeability coefficient. No work has been reported on the granular soils.

In 1987 Bamforth investigated the relationship between permeability coefficients for concrete obtained using liquid and gas and reproduced a relation similar to Klinkenberg's.

Theory of Air Flow Through Soils

Several mechanisms of fluid flow through porous materials are known to exist. The primary mechanism is, of course, of a purely "mechanical" nature, namely, flow as a result of an applied force in the form of a pressure differential. However, flow may also occur under certain circumstances as a result of applied electrical or thermal gradients as diffusion.

Laminar flow of a fluid is characterized by a fixed set of streamlines. A fluid element which at one point is traversing the same path as another element must follow the path of this element throughout its course. This is in contrast to turbulent flow in which only partial correlation between particle paths exists.

The viscosity of a fluid is a measure of internal friction associated with laminar flow. Shear forces exist apparently between lamellae of fluid having different velocities. An ideal viscous fluid flowing over a solid surface adheres to the surface. At the surface of the solid the fluid velocity is zero. As a result of this fluid sticking to the solids and the viscosity of the fluid, a drag force is exerted on the solid by the fluid. The fluid tends to drag the solid along with it.

Fig. (4) shows a cylindrical sample of porous material having parallel ends, cross-sectional area A, and length L is mounted in a tube. The walls of the tube are tightly bonded to the sample. It is assumed that the system is filled with fluid.

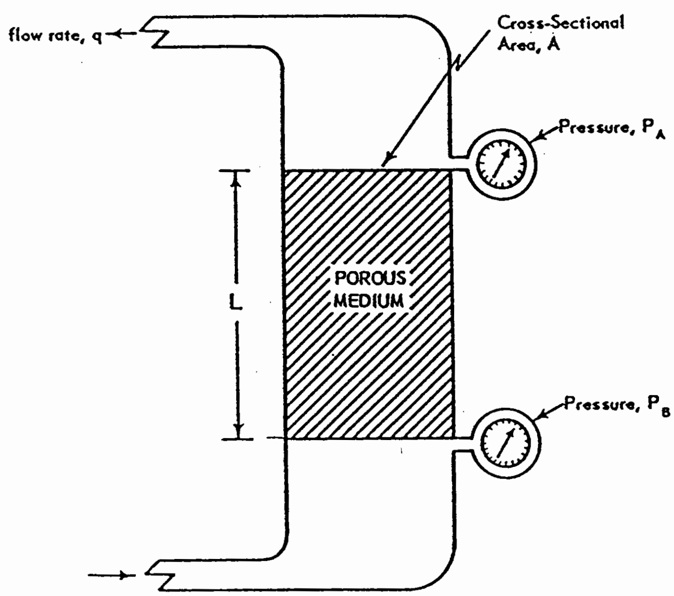

Figure 5

For flow upward through the sample a net viscous resistance directed downward opposes the flow. In principle, this force could be computed by integrating Newton's equation:

$$F_u = \mu \{dv/dz\}$$

Where "F" is the shear force per unit area between the solid surface and a fluid tangent to it, "μ" is the fluid viscosity, "v" is fluid velocity, and "z" is the distance from the surface into the fluid. It should be noted that the derivative is evaluated at the surface of the solid hence the integration is over the internal pore surface (Collins 1961). Since the geometry of the pore surface is beyond mathematical description, this cannot be done. Even so, certain facts about this force can be stated mathematically.

Since for laminar flow the relative distribution of velocity within the pores is independent of the magnitude of the velocity, it follows that "v" and hence "dv/dz" must be everywhere proportional to "q/A" where q is mean volumetric flow rate. Furthermore, since the total surface involved must be proportional to the bulk volume, "AL", of porous material, it follows that the viscous drag on the fluid can be written as:

$$F_\mu = B \mu \vec{q} L$$

Where "B" is a constant with dimensions of reciprocal length squared which is characteristic of the pore geometry. The force "F " is directed downward for upward flow.

The external forces acting on the fluid contained within the porous sample can be expressed in terms of pressures P_a and P_b at the ends of the sample. Since the pore areas on which these pressures act are given by "ηA", where "η" is the porosity of the sample, the net upward force on the fluid due to these pressures can be written as:

$$F_p = (P_b - P_a)\ \eta\ A$$

The body force on the fluid is simply the weight of the fluid in the sample which is a downward force and can be written as :

$$F_g = \rho\,(\eta A\,L)\ g$$

here "ρ" is the mass density of the fluid and "g" is the acceleration of gravity.

For steady flow, the above mentioned three forces must be in equilibrium. Thus,

$$B\,\mu\,\bar{q}\,L + \rho\,(\eta A\,L)\ g = (P_b - P_a)\,\eta\,A$$

or

$$(B/\eta)\ \mu\,\bar{q}\,L = (P_b - P_a)\ A - \rho\ (A\ L)\ g$$

so

$$\bar{q} = [(\eta/B)\ A/(\mu L)]\ \ ((P_b - P_a) - \rho\ L\ g)$$

Let $(\eta/B) = K$ (Apparent permeability "length squared")

$$\bar{q} = [-\ KA/\mu L]\ \ ((P_a - P_b) + \rho\ L\ g) \qquad \text{Eq. (1)}$$

For gases "g" is negligible and compressibility should be considered.

From ideal gas law:

$$q_a\ P_a = \bar{q}\ (P_a + P_b)/2$$

Subst. in Eq. (1) and neglect "g" term for gases:

$$q_a P_a = [- K A/ \mu L] (P^2_a - P^2_b) /2$$

Solve for "K",

$$K - (2 q_a P_a \mu L) / (P^2_b - P^2_a) A \qquad \text{Eq. (2)}$$

Equation (2) is the same equation used in the ASTM (D 4525-85) for permeability of rocks by flowing air.

<u>Laminar Viscous Flow Through Porous Media</u>

The laminar flow regime breaks down for sufficiently high flow rates. For high flow rates, Darcy's law is not valid. The range of flow rate for which laminar flow exists has been studied by numerous investigators (Ergun 1949, Fancher 1933, Dybbs and Edwards 1984). Generally, this range is defined in terms of Reynolds number. Dybbs and Edwards (1984) defined a modified Reynolds number for flow through porous media as:

$$R_e = \frac{\rho v d}{\mu} \frac{\eta}{1-\eta}$$

where "v" is the average microscopic of "pore" velocity, "d" is the pore diameter, "μ" is fluid viscosity, "ρ" is fluid density at atmospheric pressure and "η" is porosity of the porous sample.

Due to the fact that in porous media a distribution of pore sizes exists, the transition from laminar to turbulent flow is not abrupt at a critical Reynolds number as is the case for flow through pipes. Instead the transition is rather gradual. True turbulence occurs only at very high Reynolds numbers (about 700).

Most investigators agreed that the slow laminar flow regime starts to break down at Reynolds number greater than ten. Fortunately, the flow regime in most cases of practical interest is of the slow laminar type and Darcy's law applies. The mathematical theory of flow through porous media is generally formulated with Darcy's law being taken as the fundamental law of flow with some consideration to the compressibility in case of gas flow since air for example compresses 20,000 times cold water at 20'C.

Experimental Technique

Fig. (6) shows a sketch of the latest apparatus used after several trials to produce an apparatus with optimum length and cross section area since short specimen presents a statistically poor sample and long samples are difficult to handle as well as to prepare. Sampler holder was made of plexi-glass tube and the inner surface was coated with silicon cement to prevent bypass flow around the sample. The length of the apparatus is 24 inches and the inner cross section area is 4.87 inch squared.

Air is introduced to the sample in the vertical direction from an air pressure regulater connected to the compressed air supply. The entrance and exit flow ports are sufficiently large to prevent pressure loss at maximum flow rate. Pressures along the sample are measured with mercury and water manometers. The amount of air passing through the sample is measured with a flowmeter.

Five different types of soils were used in the research on Ottawa sand, concrete sand, masonry sand, silty sand, and volcanic ash. Figure (7) shows the grain size distribution for each soil using both the sieve analysis and the hydrometer approach. Soils were prepared inside the apparatus according to the latest technique known for preparing the granular soils (Rad and Tumay, 1987). Each type of soil was tested with at least three different relative densities.

Air was introduced to the sample first at maximum flow rate to prevent compressing of the soils during the test, then the length of the sample was measured. Air pressures were measured at the entrance and the exit of the device, at four ports spaced at one inch distances along the sample length and near the flowmeter to investigate the change of the pressure with length. In the second step the flow rate was reduced and measurement of air pressures were taken. The pressure was reduced and the permeability measured until zero flow rate was almost reached. It should be mentioned that the flow in all steps was maintained at the steady state condition during measurement. The data were then input to a small computer program using spread sheet software to compute the air permeability of the soils. Finally, using Klinkenberg theory, the measurements at finite mean pressures are extrapolated to infinity and the true intrinsic permeability (K_s) of the soil is obtained. Some of the typical results and computer out put is presented in the appendix. The hydraulic permeability coefficient (k_w) of the soil is computed by multiplying the intrinsic permeability (K_s) by the water density (γ_w) and then dividing the result by the water viscosity (μ) $\{K_s = k \ \mu/\gamma_w\}$ (Lambe and Whitman 1979).

Modification for the Flow of Air Equation

In deriving the equation $K = (2\ q_a\ P_a\ \mu\ L)\ /\ (P_b - P_a)\ A$ Eq. (2), we assumed that the pressure of air is changing linearly with depth but experimental results showed that the pressure in most cases is not changing linearly with depth of soil due to the fact the soil is neither

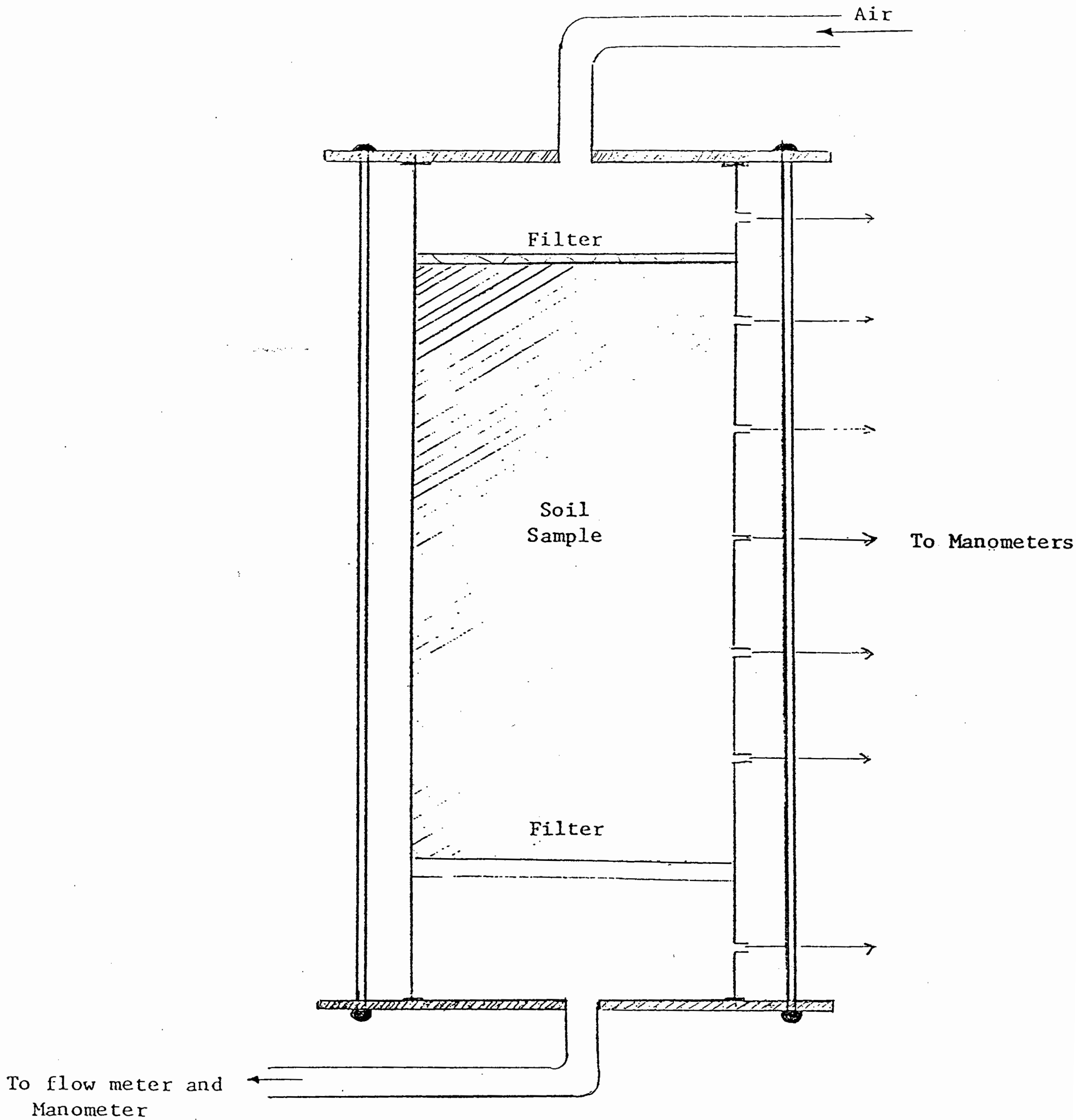

The Apparatus

Figure 6

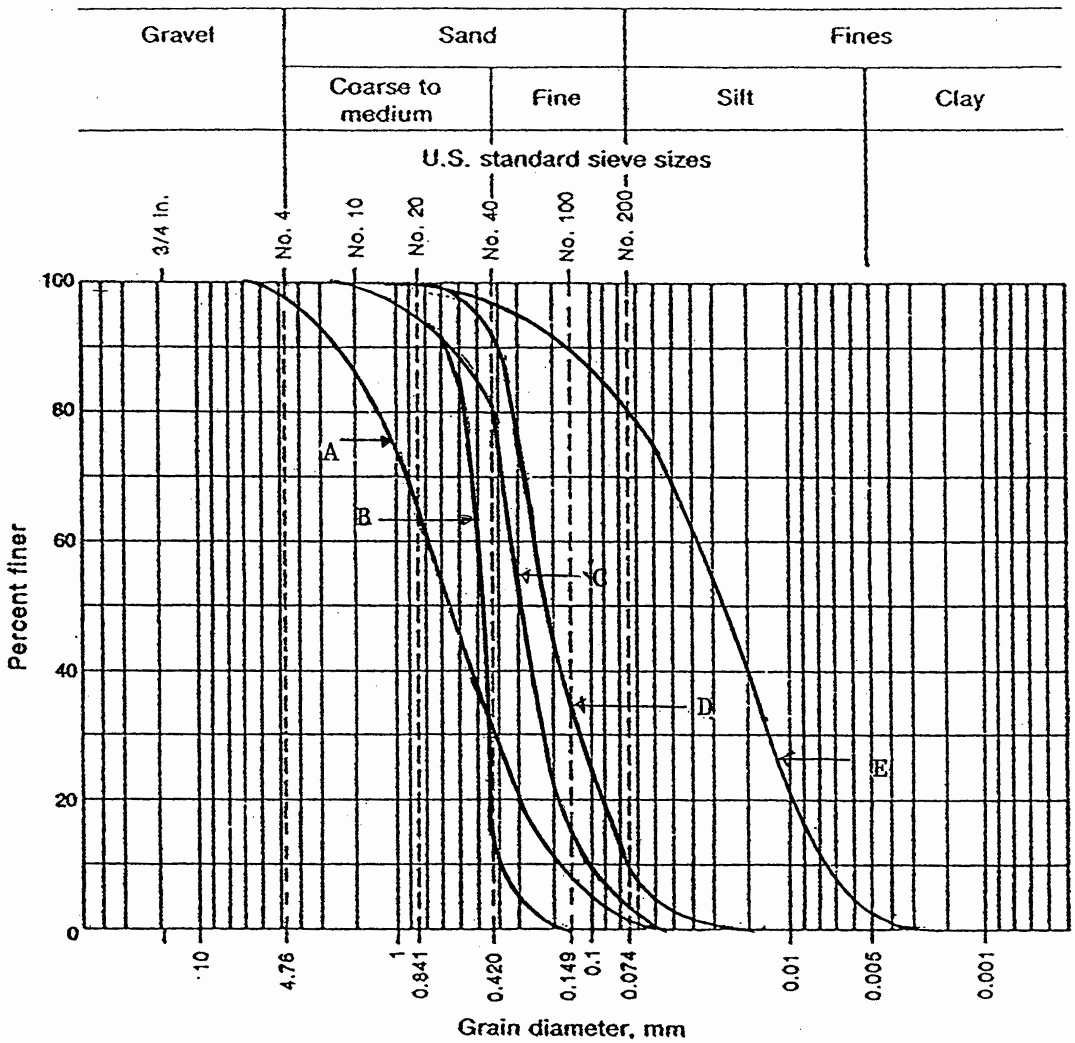

Grain Size Distribution for Tested Soils.

A = Concrete sand B = Ottawa sand

C = Masonary sand D = Silty sand

E = Volcaic ash

Figure 7

homogeneous nor istropic. Fig. (8) through Fig. (11) show typical curves of the variation of the pressure with the length of the sample. For this reason the mean pressure "P_m" was approximated using the trapezoids rule. It was found also that "P_a" in the manometer is not necessarily the same as the pressure near the flowmeter; hence we introduce a new term called "P_f" which is the air pressure near the flowmeter. The final equation used to compute the apparent permeability can be written as:

$$K = (q_a \; P_f \; \mu \; L) \; / \; (P_b - P_a) \; P_m \; A \qquad \text{Eq. (3)}$$

Results

Figures (12) through (24) show the results for testing different types of soil: volcanic ash, silty sand, masonry sand, concrete sand and Ottawa sand. As can be seen from these figures, the data plots as a straight line. Also Figures (25) to (27) show the effect of changing the porosity and the relative density on the permeability of the silty sand, masonry sand and concrete sand respectively. It is clear from Figures (23) and (24) [Ottawa sand] that Klinkenberg theory does not apply for highly permeable materials since at high flow rates the laminar flow regime breaks down and Darcy's law is not valid. For this reason there is difference between the dotted line in Figure (23) (which represents the changing of the permeability with ($1/p_m$) assuming laminar flow), and the solid line (which is the actual one). This difference increases when the mean pressure increases ($1/p_m \approx 0$) due to the fact that turbulent flow increases at high flow rate. It should be mentioned that in turbulent flow, momentum exchange is the basis of shear resistance; it occurs on macroscopic scale, being caused by random fluctuations in velocity which

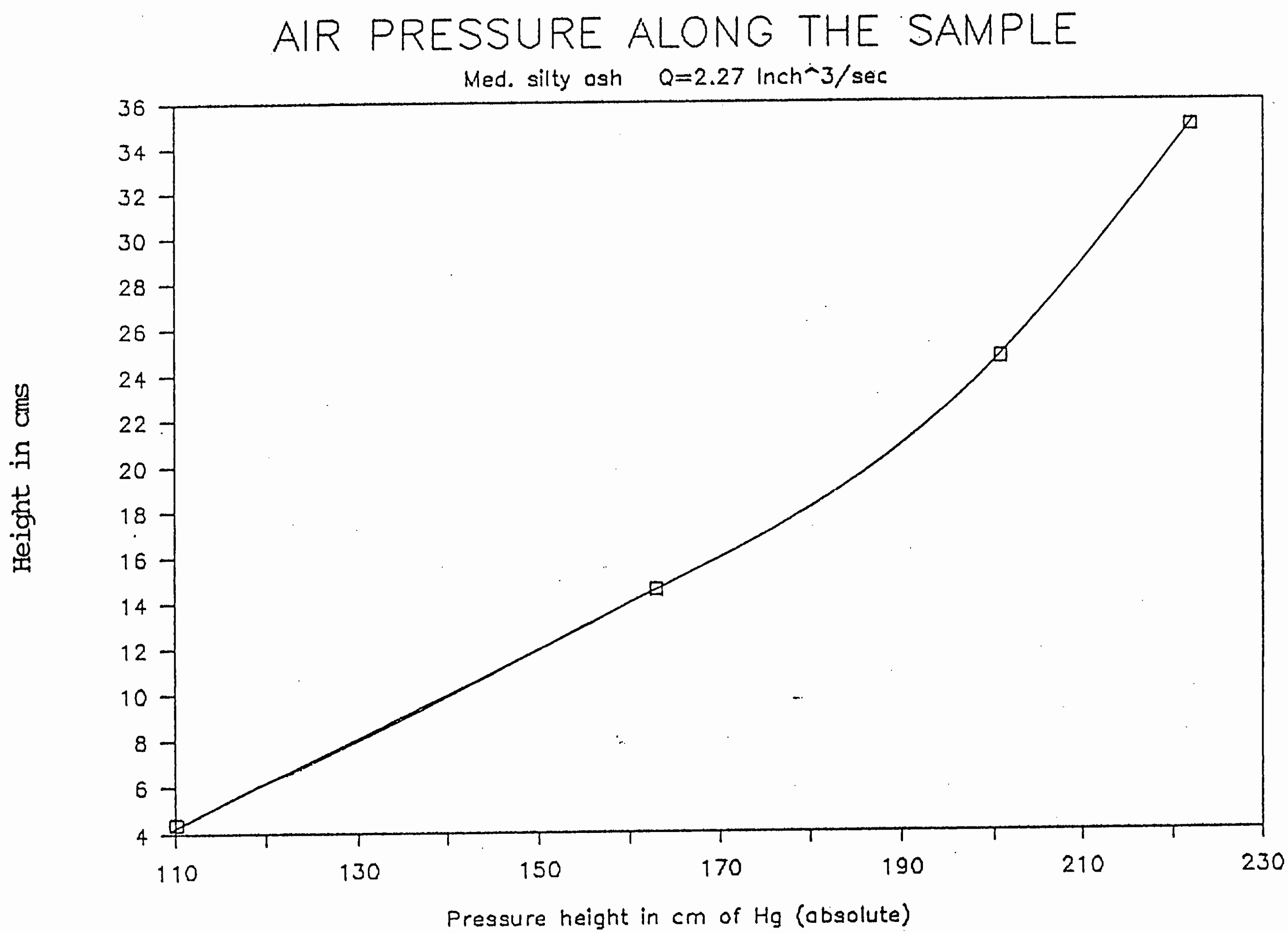
AIR PRESSURE ALONG THE SAMPLE
Med. silty ash Q=2.27 Inch^3/sec
Height in cms
36
34
32
30
28
26
24
22
20
18
16
14
12
10
8
6
4
110
130
150
170
190
210
230
Pressure height in cm of Hg (absolute)

Figure 8

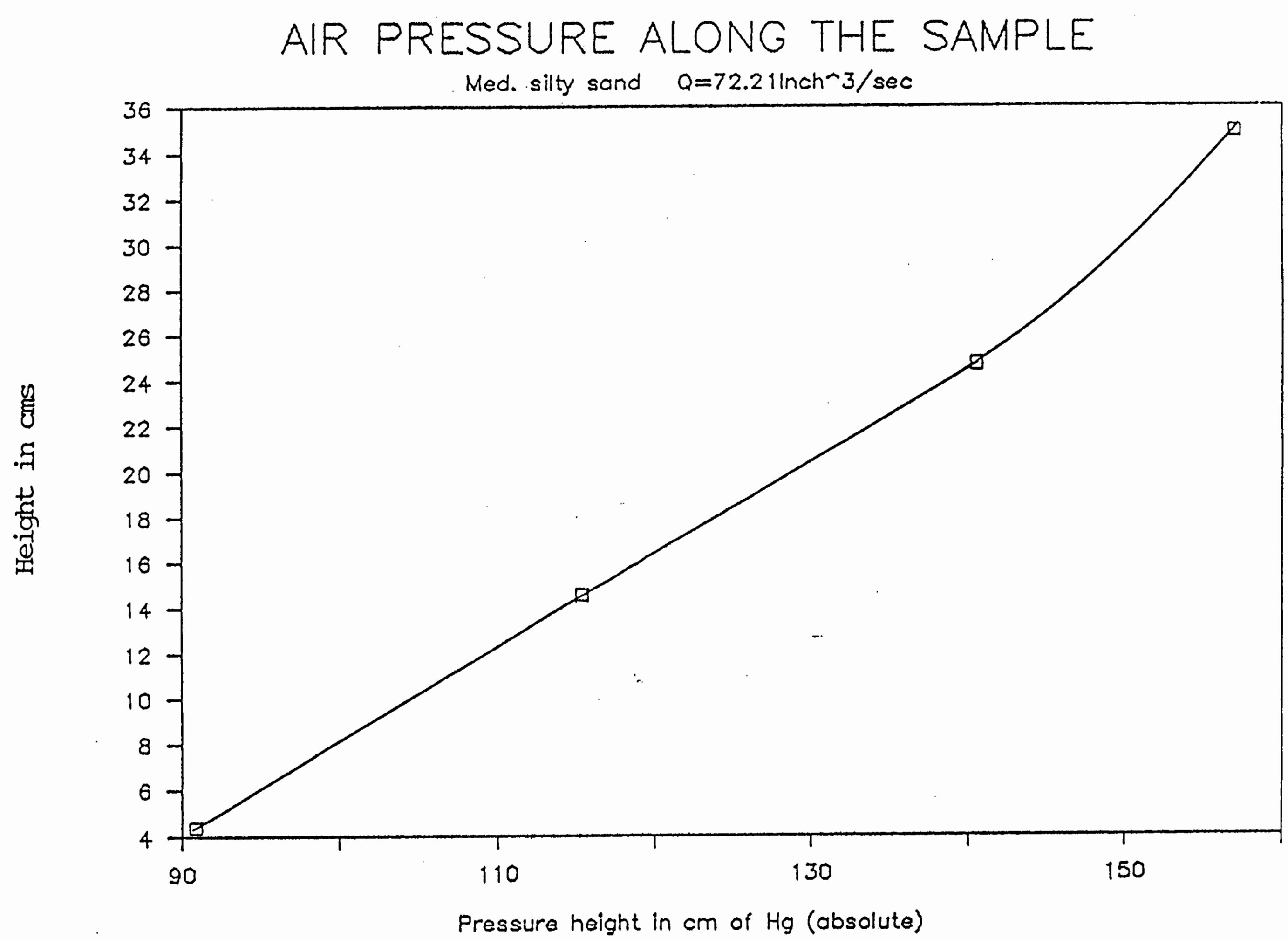
AIR PRESSURE ALONG THE SAMPLE
Med. silty sand Q=72.21Inch^3/sec
Height in cms
36
34
32
30
28
26
24
22
20
18
16
14
12
10
8
6
4
90
110
130
150
Pressure height in cm of Hg (absolute)

Figure 9

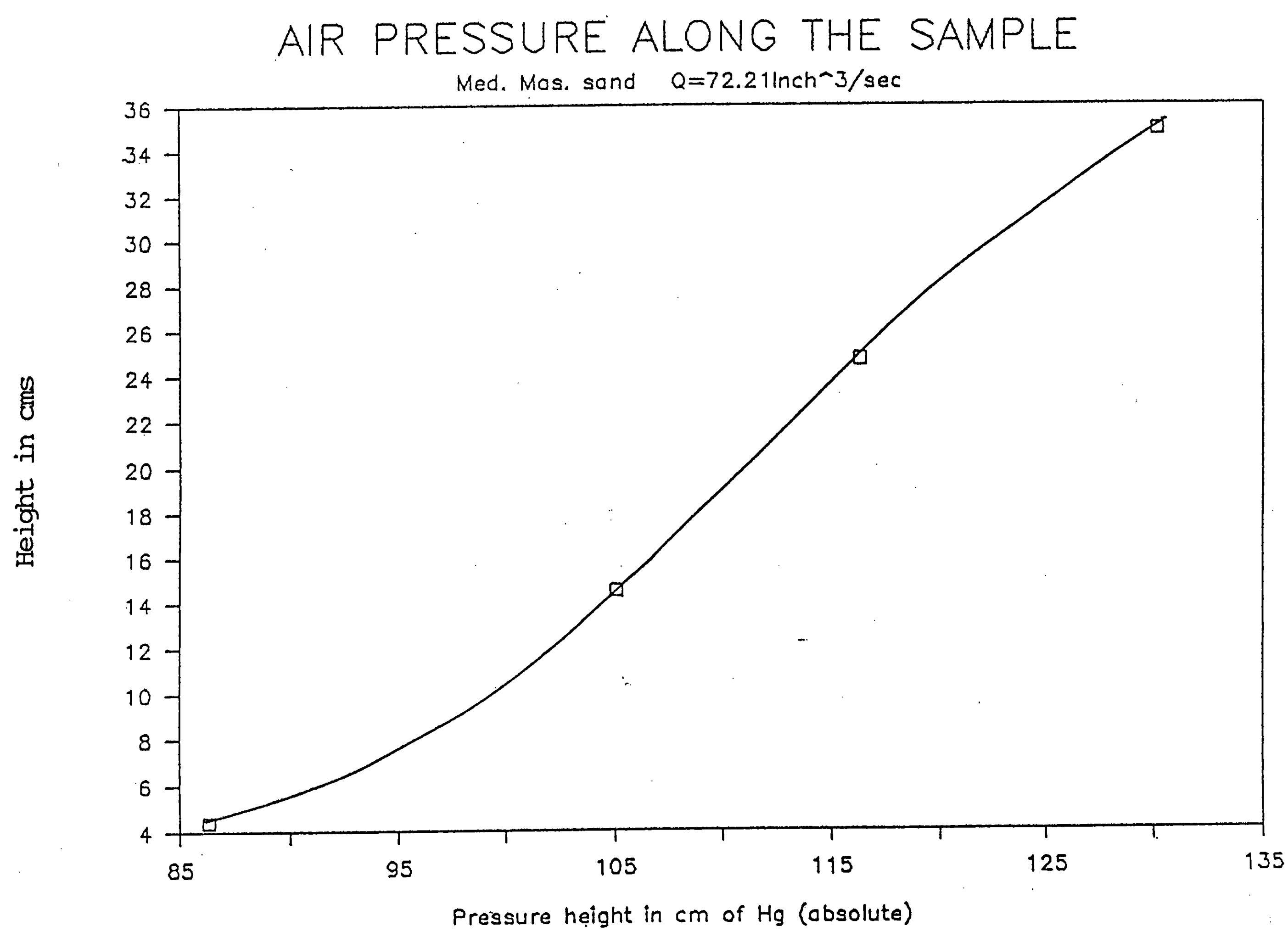
AIR PRESSURE ALONG THE SAMPLE
Med. Mas. sand Q=72.21Inch^3/sec
36
34
32
30
28
26
24
22
20
18
16
14
12
10
8
6
4
Height in cms
85
95
105
115
125
135
Pressure height in cm of Hg (absolute)

Figure 10

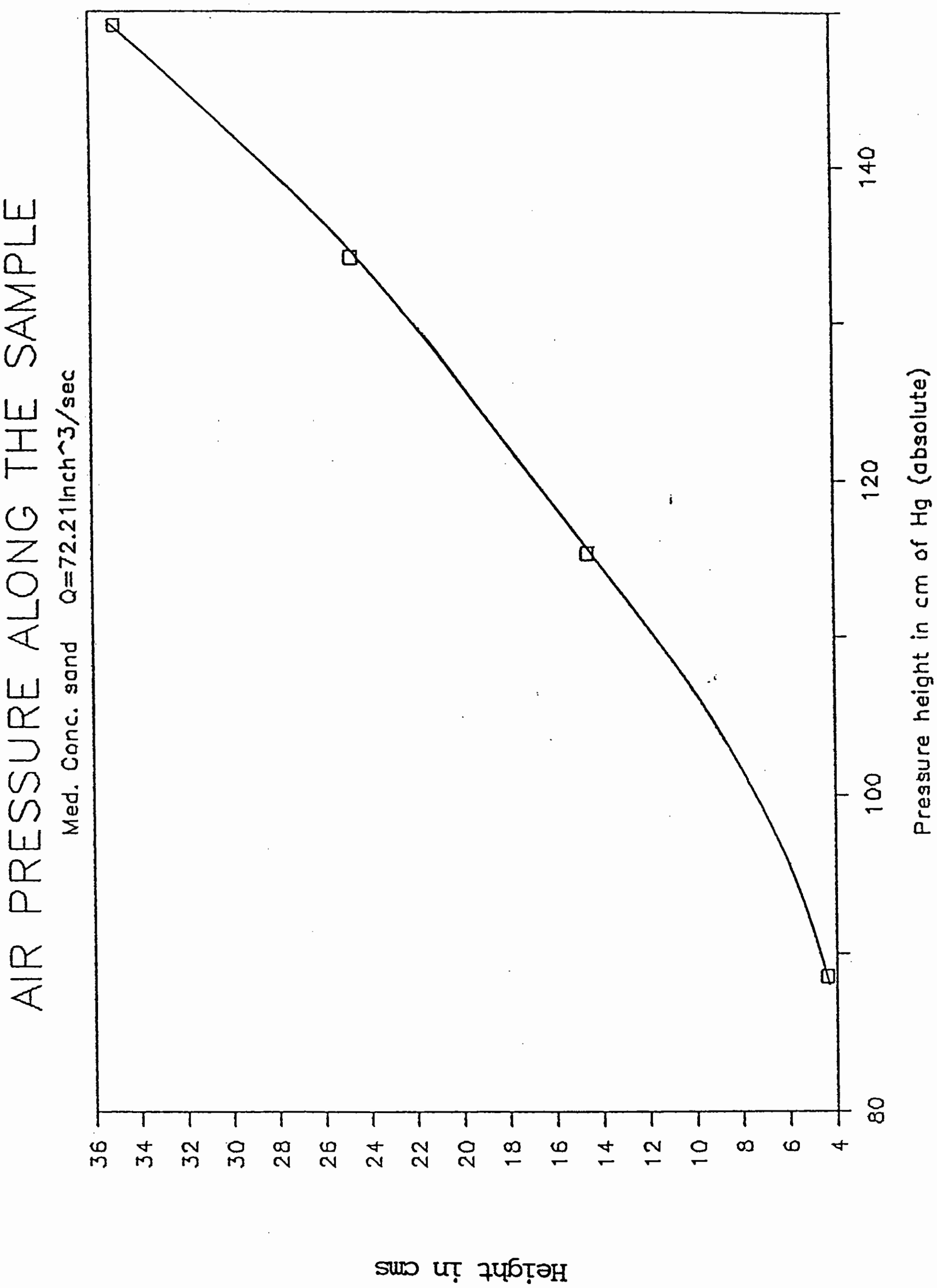
AIR PRESSURE ALONG THE SAMPLE
Med. Conc. sand Q=72.21Inch^3/sec
Height in cms
36
34
32
30
28
26
24
22
20
18
16
14
12
10
8
6
4
80
100
120
140
Pressure height in cm of Hg (absolute)

Figure 11

are continually sending fluid particles back and forth between adjacent layers. This increase of the shear resistance is the reason for decreasing the apparent permeability coefficient in Fig. (24).

Hydraulic permeabilities of soils were measured using the falling head method for different types of soils with varying relative density. Soils were saturated first with water so the comparison between the hydraulic permeability extrapolated from air flow test and the hydraulic permeability obtained from water flow test is under the same condition of saturation with air and water respectively. Figures (28) to (31) show the results of the hydraulic permeability test using the falling head method for each soil under packing conditions of different density.

Comparison between the hydraulic permeability coefficients obtained by air flow and water flow method is shown in Table 1. Also Table 1 shows the void ratio, relative density, Reynolds number and the absolute permeability for each sample.

Table 1

Sample	Void ratio e	Dr %	K_s (b) $Inch^2$	slope (a) Pounds	K_{water} Calculated from K_s cm/sec	K_{water} Measured cm/sec	Ratio*	(Modified) Reynold's number
Volcanic Ash	1.178	-	$.025 \times 10^{-8}$	$.197 \times 10^{-8}$	16×10^{-5}	8.5×10^{-5}	1.88	0.03
Dense Conc. Sand	0.35	86	0.73×10^{-8}	15.14×10^{-8}	4.74×10^{-3}	11×10^{-3}	0.43	14.45
Medium Conc. Sand	0.54	28	1.07×10^{-8}	35.30×10^{-8}	7.01×10^{-3}	35×10^{-3}	0.20	15.93
Loose Conc. Sand	0.59	12	1.21×10^{-8}	36.74×10^{-8}	7.9×10^{-3}	45×10^{-3}	0.18	16.47
Dense Silty Sand	0.52	87	0.66×10^{-8}	3.58×10^{-8}	4.3×10^{-3}	2.2×10^{-3}	2.00	6.45
Medium Silty Sand	0.60	65	1.37×10^{-8}	22.1×10^{-8}	8.9×10^{-3}	4.5×10^{-3}	1.98	6.90
Loose Silty Sand	0.79	10	1.86×10^{-8}	40.48×10^{-8}	12×10^{-3}	10×10^{-3}	1.20	7.85
Dense Mason.Sand	0.58	79	1.62×10^{-8}	28.30×10^{-8}	1.06×10^{-2}	0.66×10^{-2}	1.60	8.09
Loose Mason.Sand	0.80	17	2.59×10^{-8}	94.69×10^{-8}	1.69×10^{-2}	1.4×10^{-2}	1.20	9.39
Dense Ottawa Sand	0.54							32.70
Loose Ottawa Sand	0.678		23×10^{-8}**			6.1×10^{-2}		35.93

*Ratio = The ratio between hydraulic permeability calculated from air permeability and hydraulic permeability by following head method.

** Measured from water test

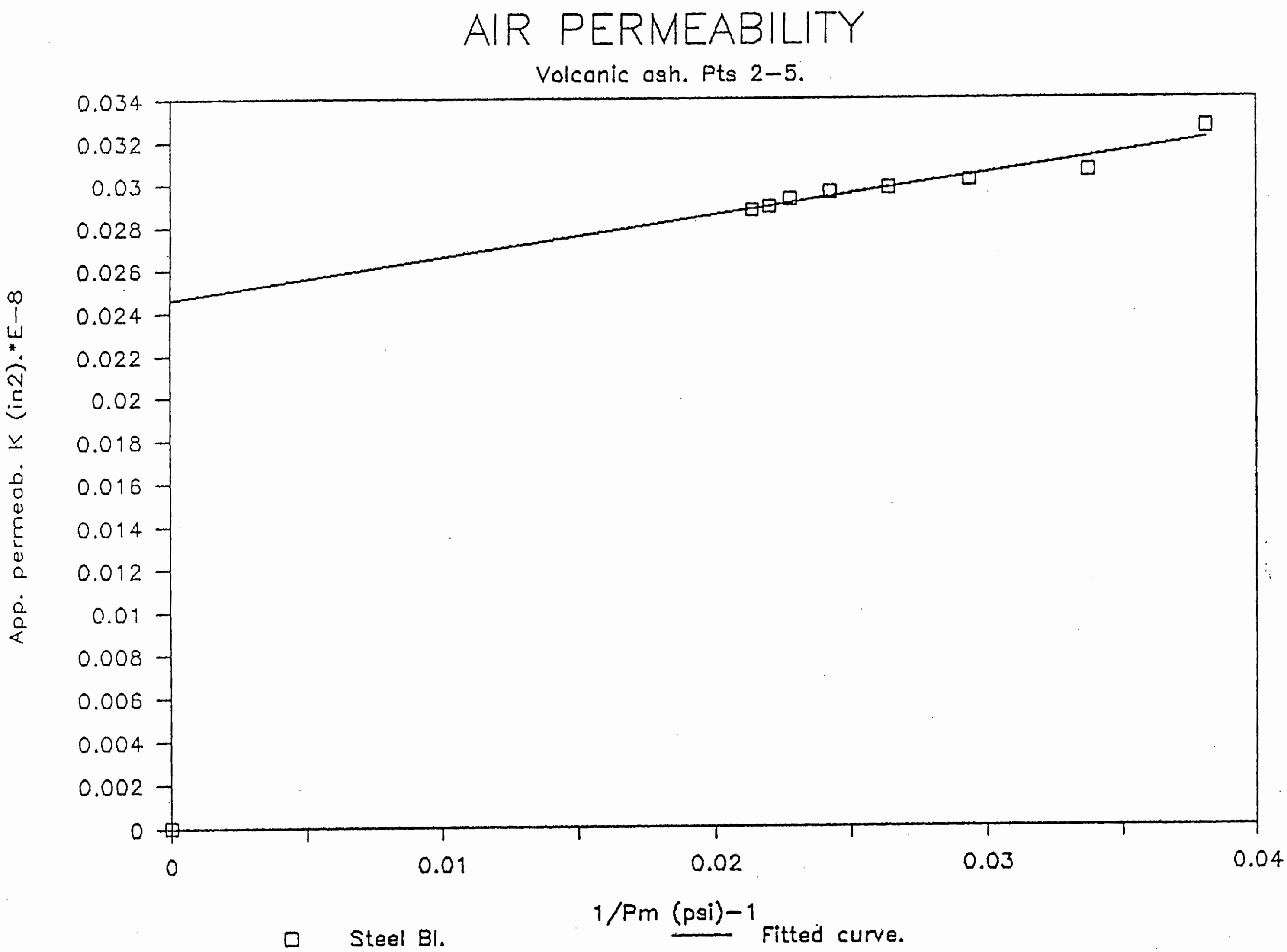
AIR PERMEABILITY
Volcanic ash. Pts 2–5.
App. permeab. K (in2).*E–8
0.034
0.032
0.03
0.028
0.026
0.024
0.022
0.02
0.018
0.016
0.014
0.012
0.01
0.008
0.006
0.004
0.002
0
0.01
0.02
0.03
0.04
1/Pm (psi)–1
Steel Bl.
Fitted curve.

Figure 12

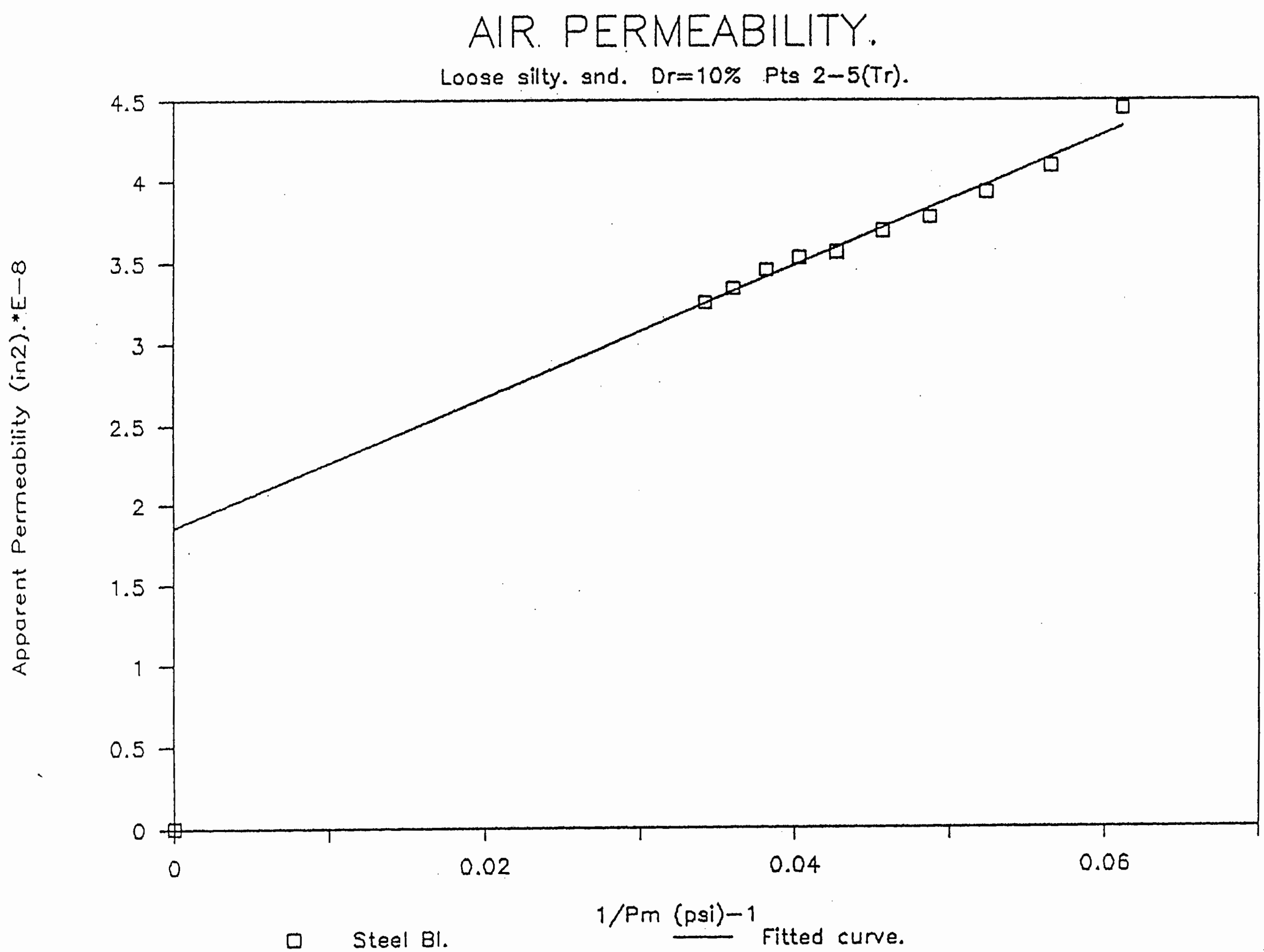
AIR PERMEABILITY.
Loose silty. snd. Dr=10% Pts 2-5(Tr).
Apparent Permeability (in2).*E-8
0
0.5
1
1.5
2
2.5
3
3.5
4
4.5
0
0.02
0.04
0.06
1/Pm (psi)-1
Steel Bl.
Fitted curve.

Figure 13

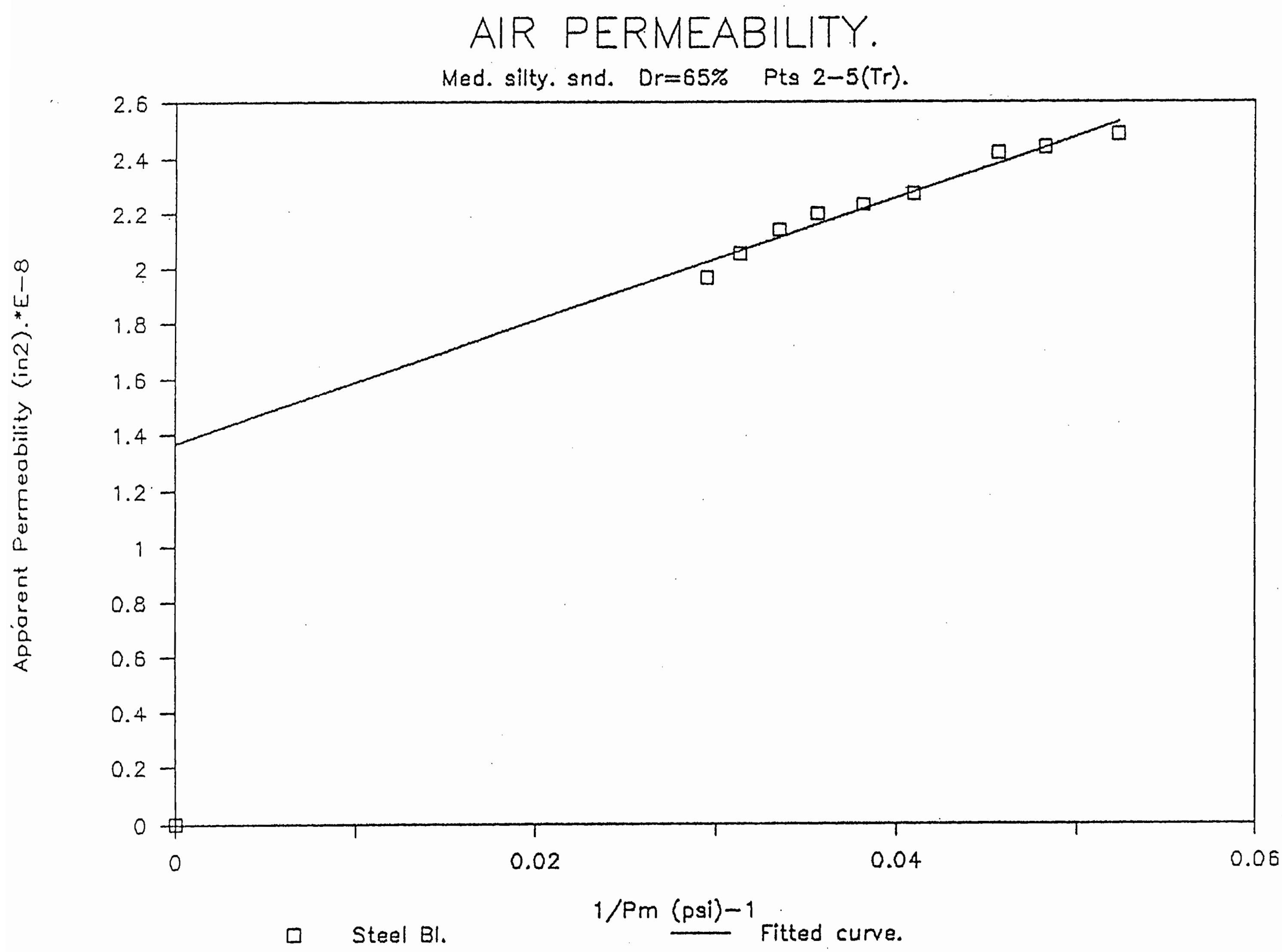
AIR PERMEABILITY.
Med. silty. snd. Dr=65% Pts 2-5(Tr).
Apparent Permeability (in2).*E-8
2.6
2.4
2.2
2
1.8
1.6
1.4
1.2
1
0.8
0.6
0.4
0.2
0
0
0.02
0.04
0.06
1/Pm (psi)-1
Steel Bl.
Fitted curve.

Figure 14

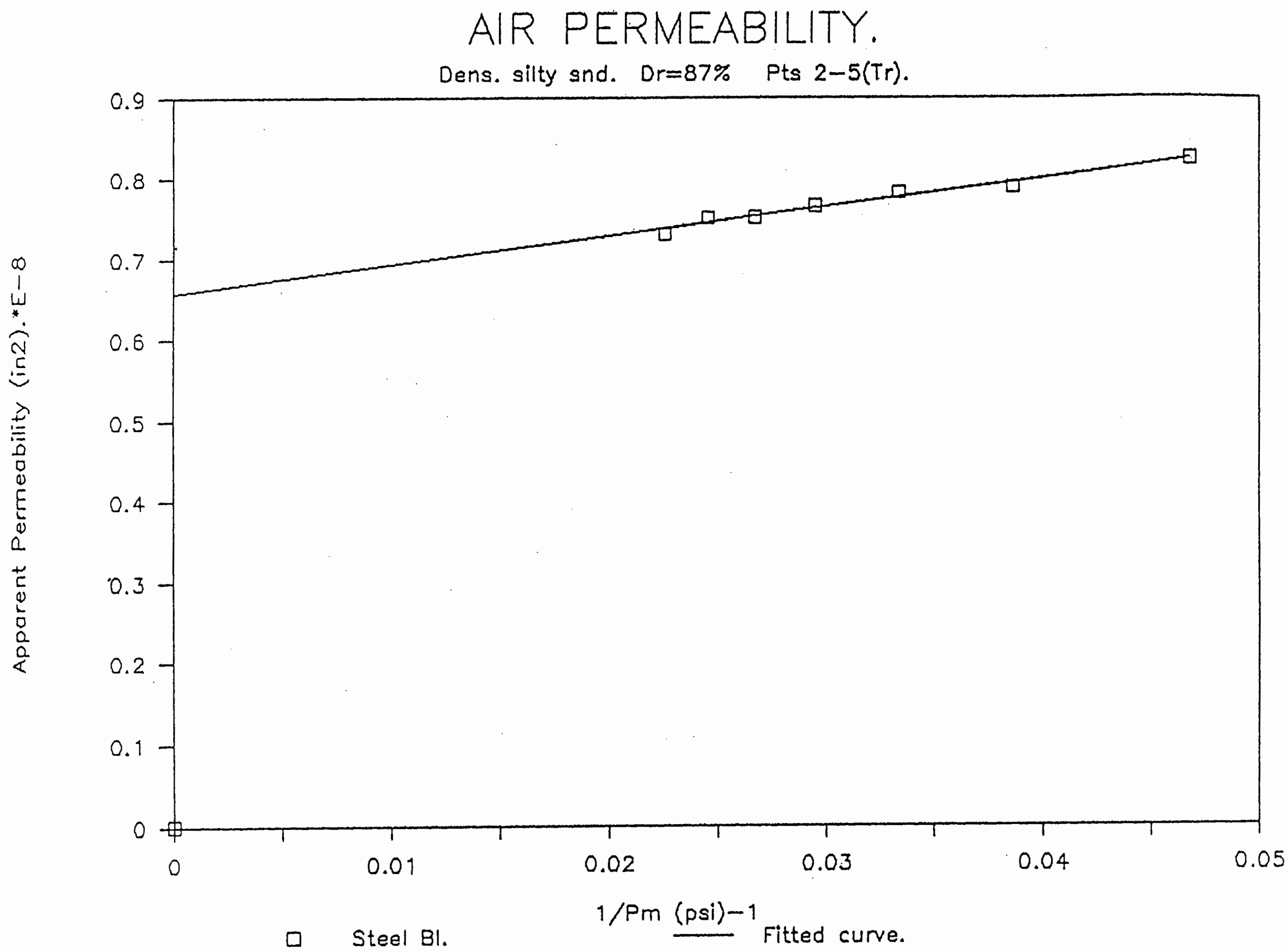
AIR PERMEABILITY.
Dens. silty snd. Dr=87% Pts 2-5(Tr).
Apparent Permeability (in2).*E-8
0.9
0.8
0.7
0.6
0.5
0.4
0.3
0.2
0.1
0
0.01
0.02
0.03
0.04
0.05
1/Pm (psi)-1
Steel Bl.
Fitted curve.

Figure 15

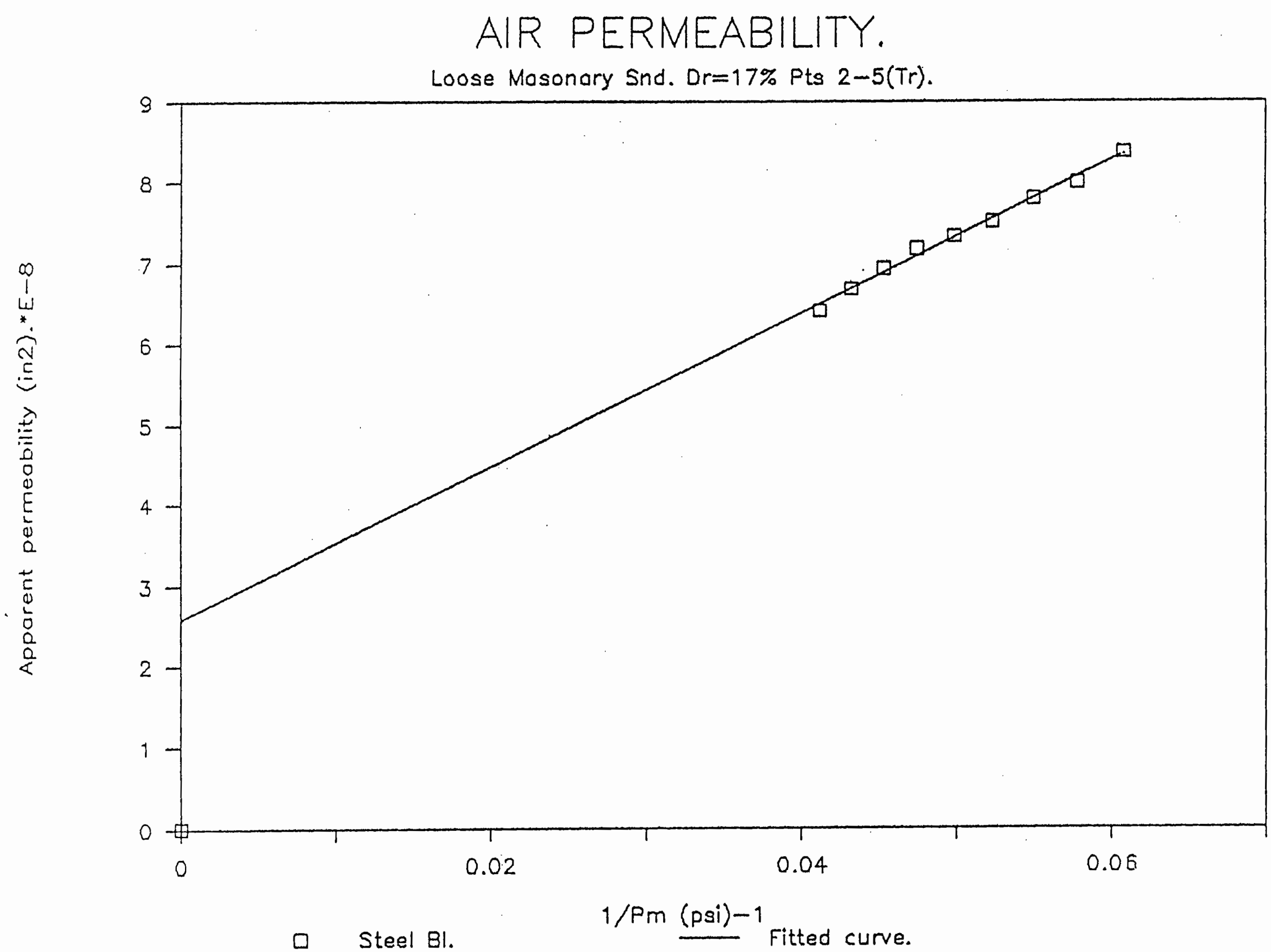
AIR PERMEABILITY.
Loose Masonary Snd. Dr=17% Pts 2-5(Tr).
Apparent permeability (in2).*E-8
0
1
2
3
4
5
6
7
8
9
0
0.02
0.04
0.06
1/Pm (psi)-1
Steel Bl.
Fitted curve.

Figure 16

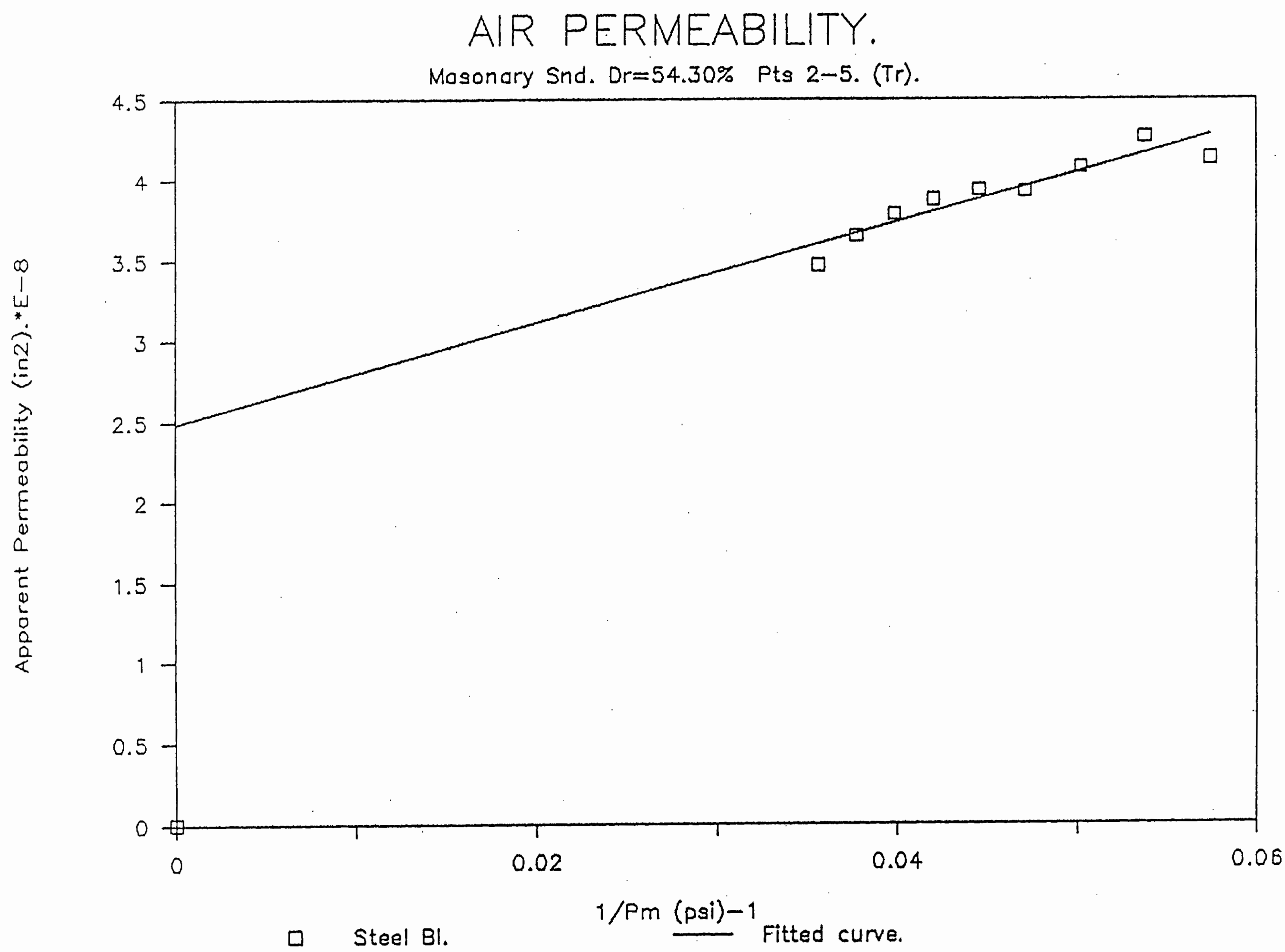
AIR PERMEABILITY.
Masonary Snd. Dr=54.30% Pts 2-5. (Tr).
Apparent Permeability (in2).*E-8
4.5
4
3.5
3
2.5
2
1.5
1
0.5
0
0
0.02
0.04
0.06
1/Pm (psi)-1
Steel Bl.
Fitted curve.

Figure 17

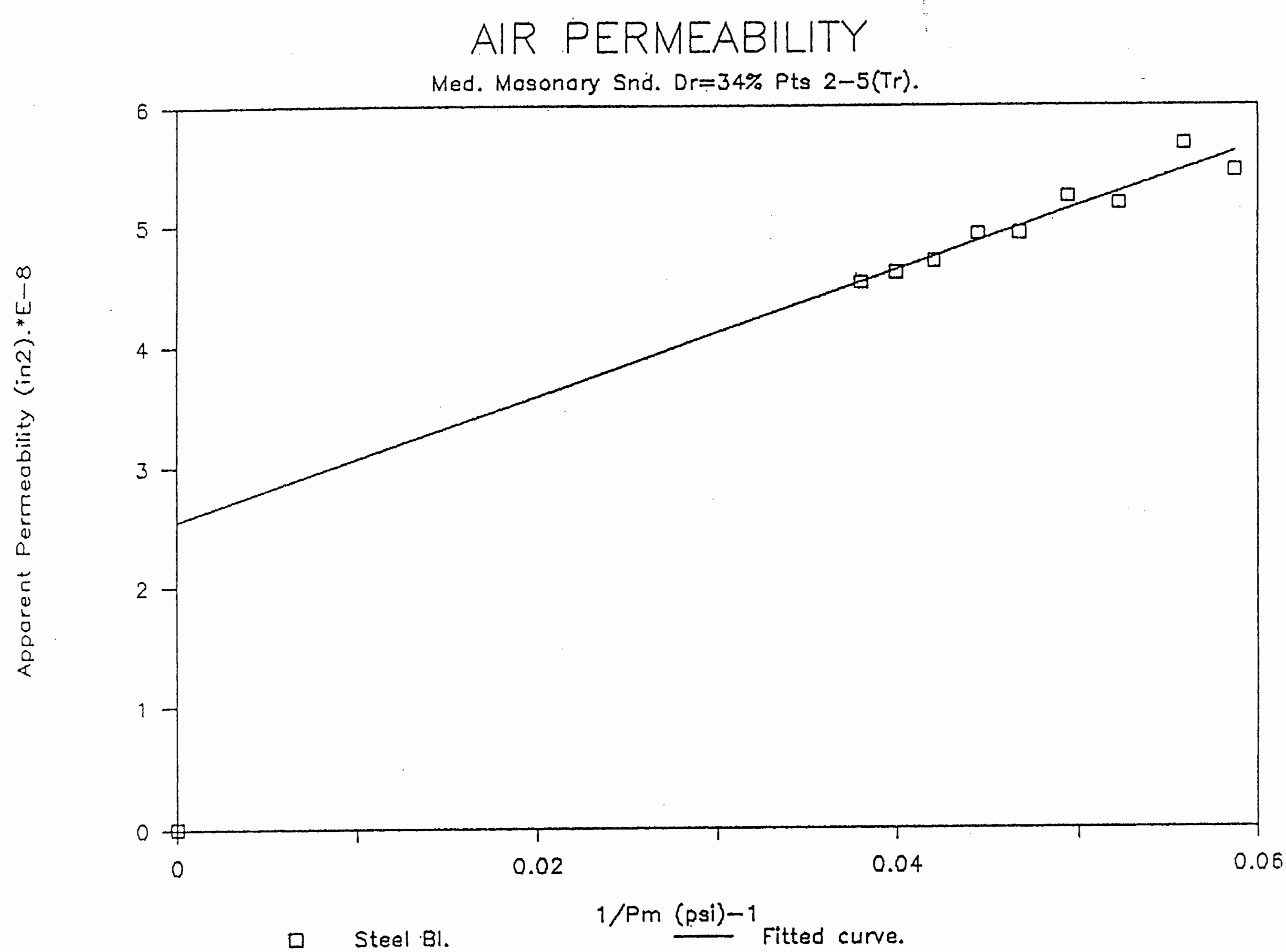
AIR PERMEABILITY
Med. Masonary Snd. Dr=34% Pts 2-5(Tr).
Apparent Permeability (in2).*E-8
0
1
2
3
4
5
6
0
0.02
0.04
0.06
1/Pm (psi)-1
Steel Bl.
Fitted curve.

Figure 18

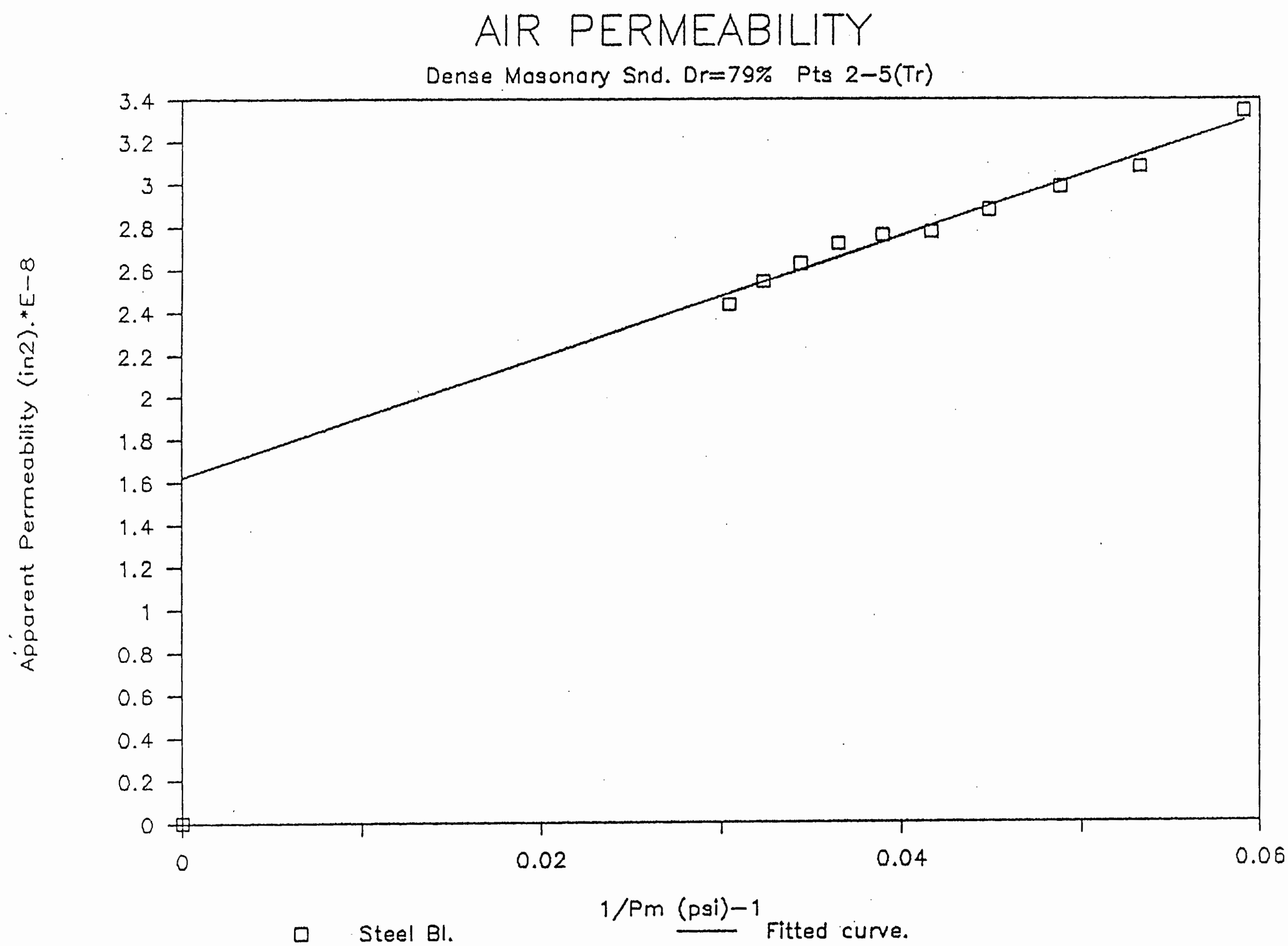
AIR PERMEABILITY
Dense Masonary Snd. Dr=79% Pts 2-5(Tr)
Apparent Permeability (in2).*E-8
3.4
3.2
3
2.8
2.6
2.4
2.2
2
1.8
1.6
1.4
1.2
1
0.8
0.6
0.4
0.2
0
0
0.02
0.04
0.06
1/Pm (psi)-1
Steel Bl.
Fitted curve.

Figure 19

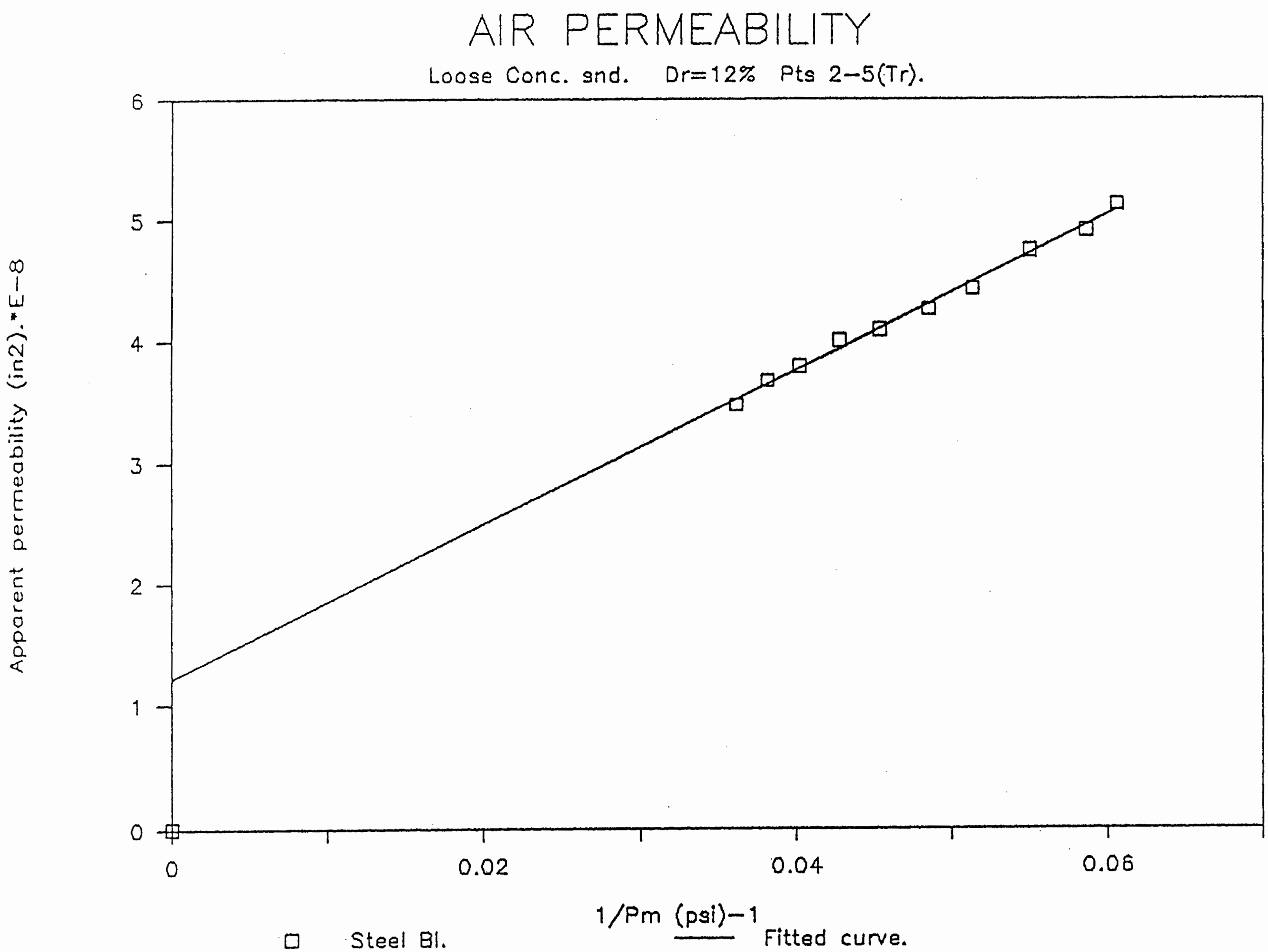
AIR PERMEABILITY
Loose Conc. snd. Dr=12% Pts 2-5(Tr).
Apparent permeability (in2).*E-8
6
5
4
3
2
1
0
0
0.02
0.04
0.06
1/Pm (psi)-1
Steel Bl.
Fitted curve.

Figure 20

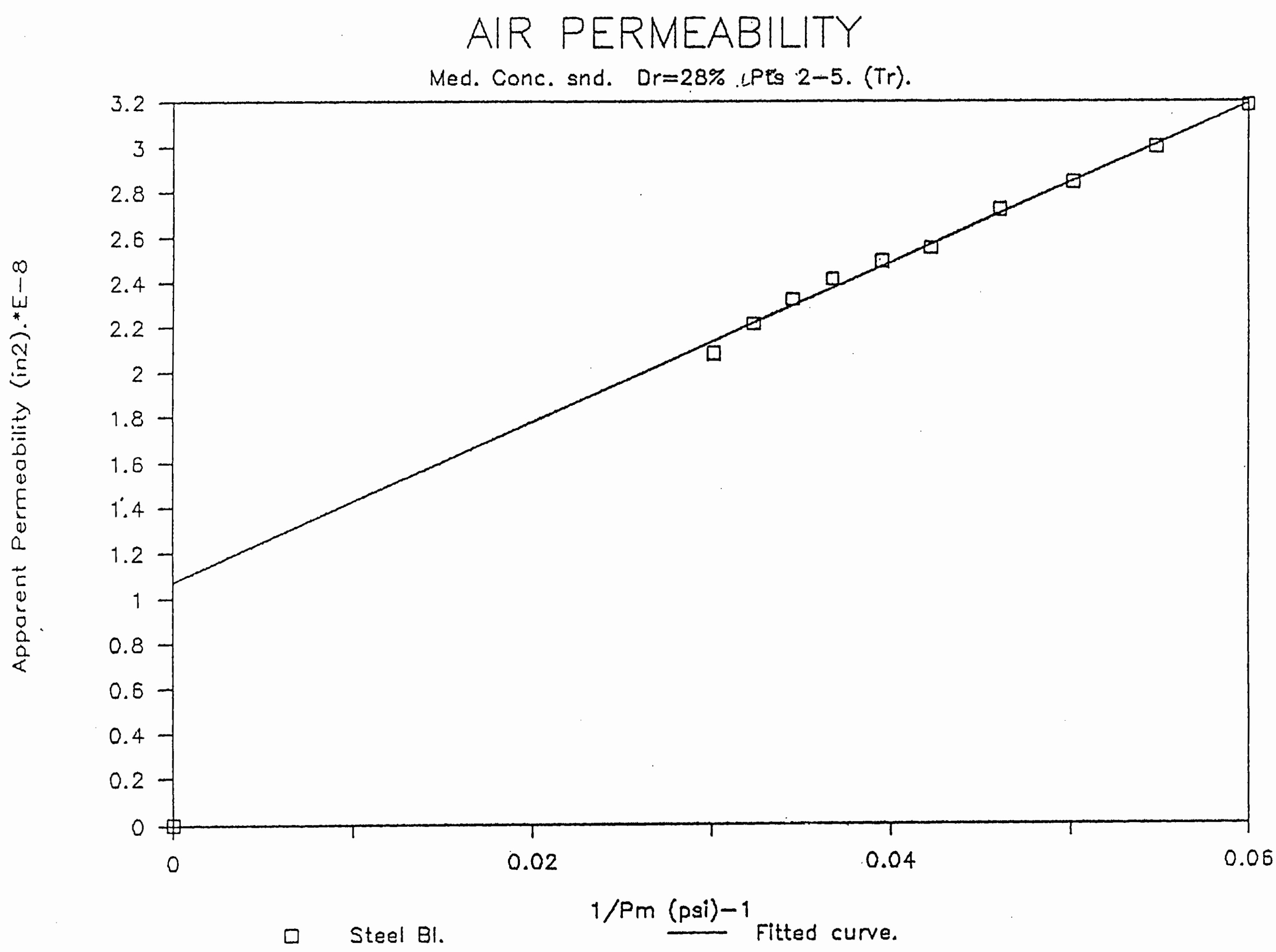
AIR PERMEABILITY
Med. Conc. snd. Dr=28% Pts 2-5. (Tr).
Apparent Permeability (in2).*E-8
3.2
3
2.8
2.6
2.4
2.2
2
1.8
1.6
1.4
1.2
1
0.8
0.6
0.4
0.2
0
0
0.02
0.04
0.06
1/Pm (psi)-1
Steel Bl.
Fitted curve.

Figure 21

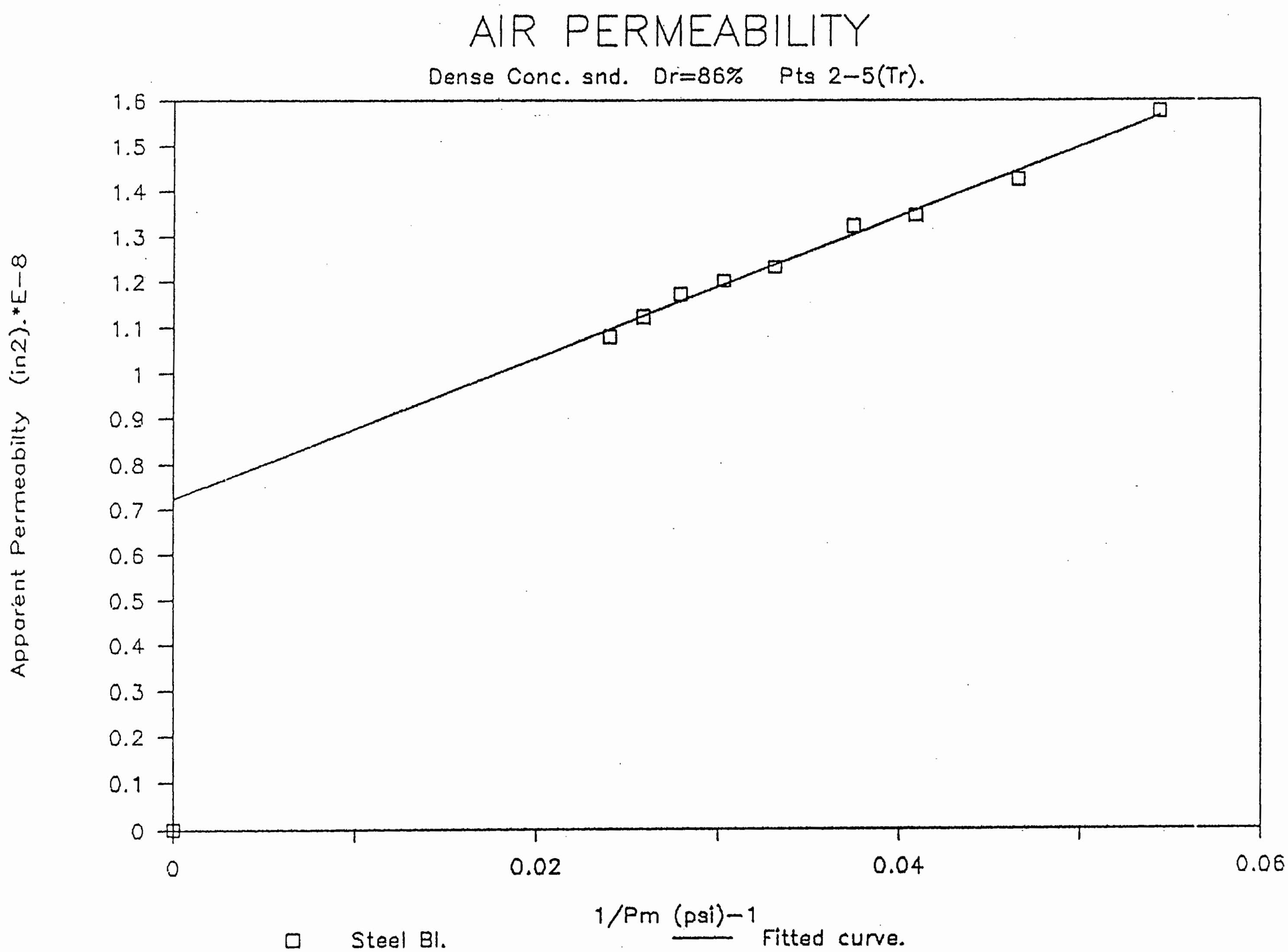

AIR PERMEABILITY
Dense Conc. snd. Dr=86% Pts 2-5(Tr).
Apparent Permeability (in2).*E-8
1.6
1.5
1.4
1.3
1.2
1.1
1
0.9
0.8
0.7
0.6
0.5
0.4
0.3
0.2
0.1
0
0.02
0.04
0.06
1/Pm (psi)-1
Steel Bl.
Fitted curve.

Figure 22

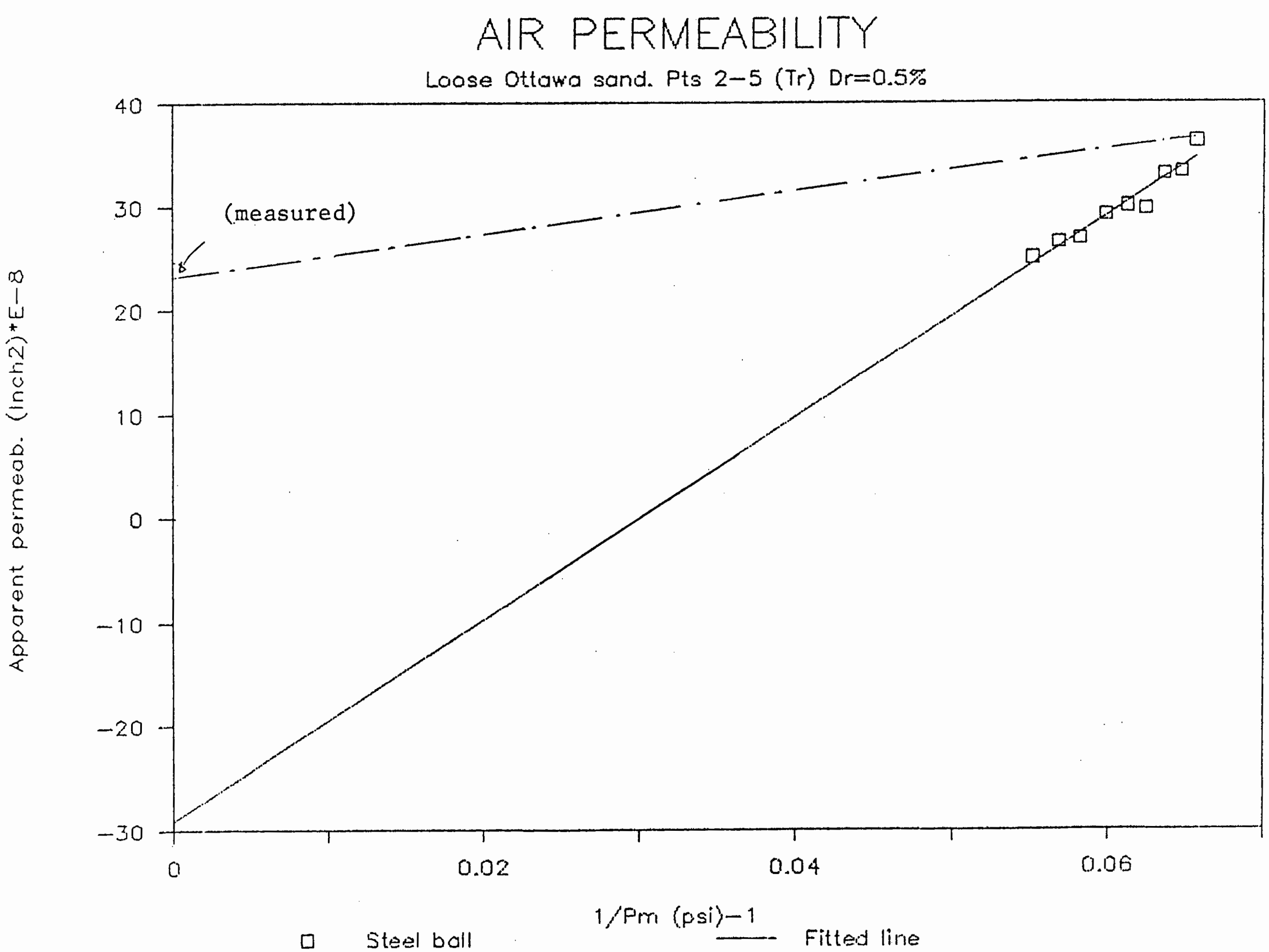
AIR PERMEABILITY
Loose Ottawa sand. Pts 2–5 (Tr) Dr=0.5%
Apparent permeab. (Inch2)*E–8
40
30
20
10
0
–10
–20
–30
0
0.02
0.04
0.06
1/Pm (psi)–1
(measured)
Steel ball
Fitted line

Figure 23

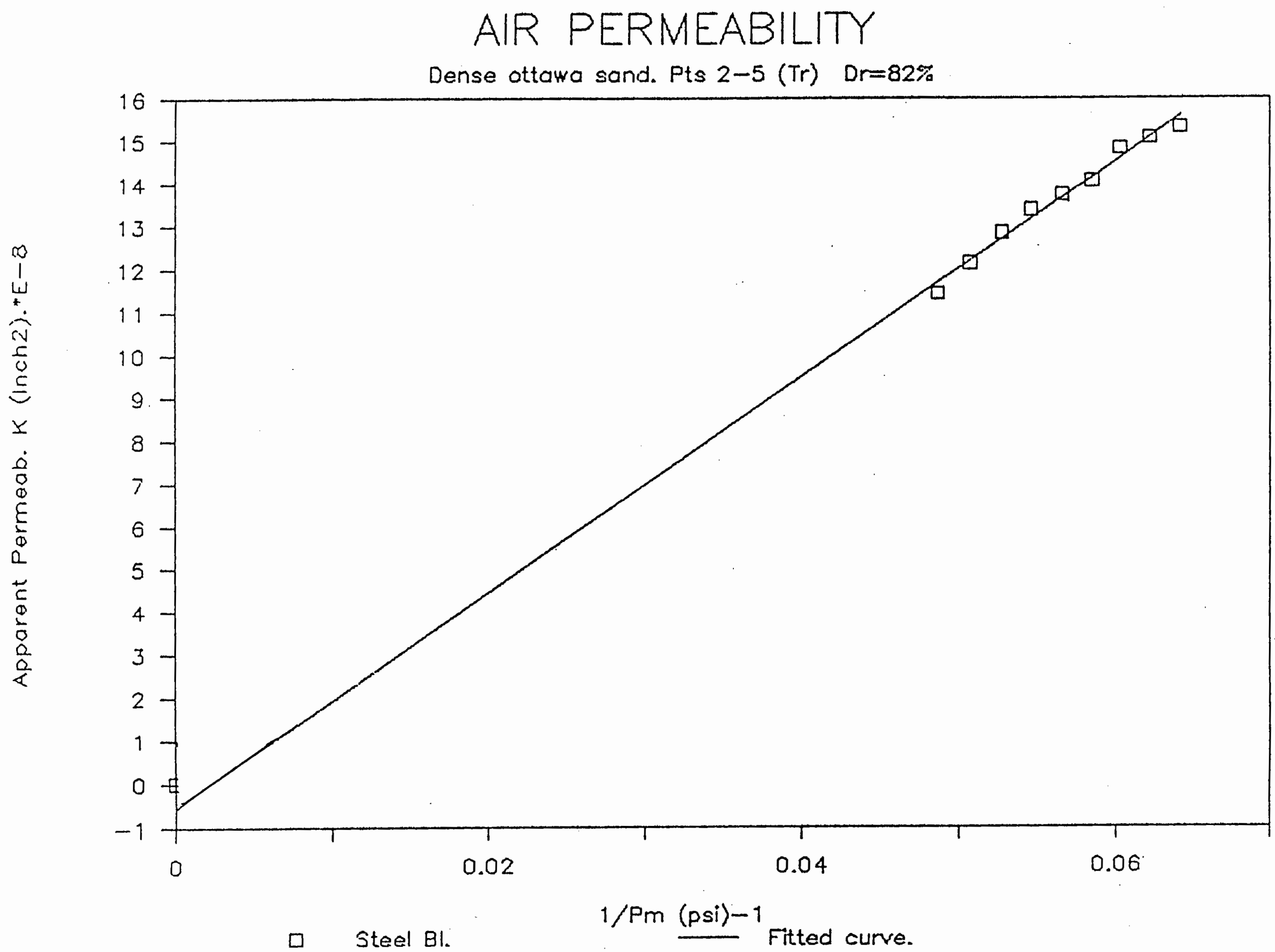
AIR PERMEABILITY
Dense ottawa sand. Pts 2–5 (Tr) Dr=82%
Apparent Permeab. K (Inch2).*E–8
16
15
14
13
12
11
10
9
8
7
6
5
4
3
2
1
0
–1
0
0.02
0.04
0.06
1/Pm (psi)–1
Steel Bl.
Fitted curve.

Figure 24

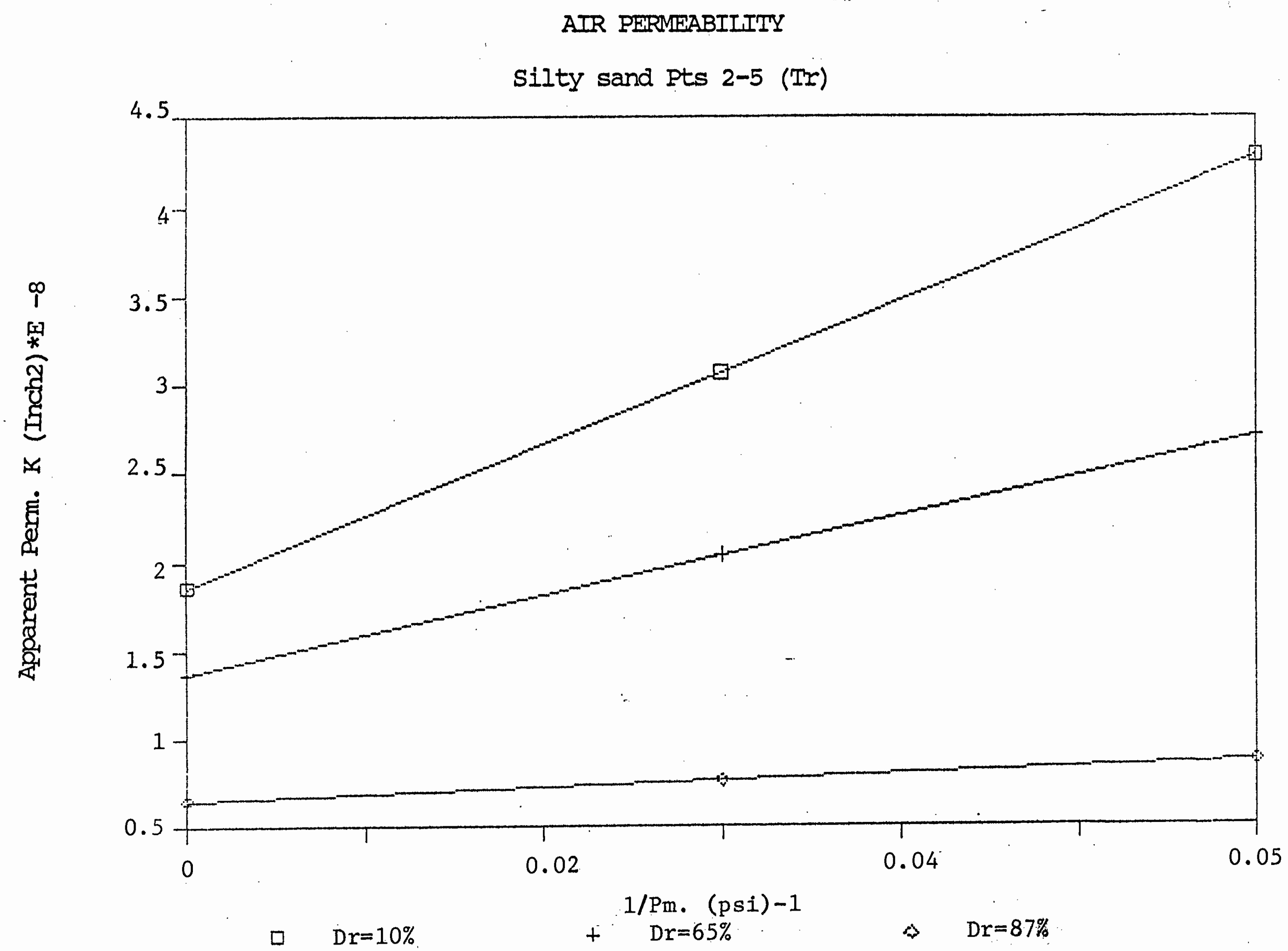
AIR PERMEABILITY
Silty sand Pts 2-5 (Tr)
Apparent Perm. K (Inch2)*E -8
4.5
4
3.5
3
2.5
2
1.5
1
0.5
0
0.02
0.04
0.05
1/Pm. (psi)-1
Dr=10%
Dr=65%
Dr=87%

Figure 25

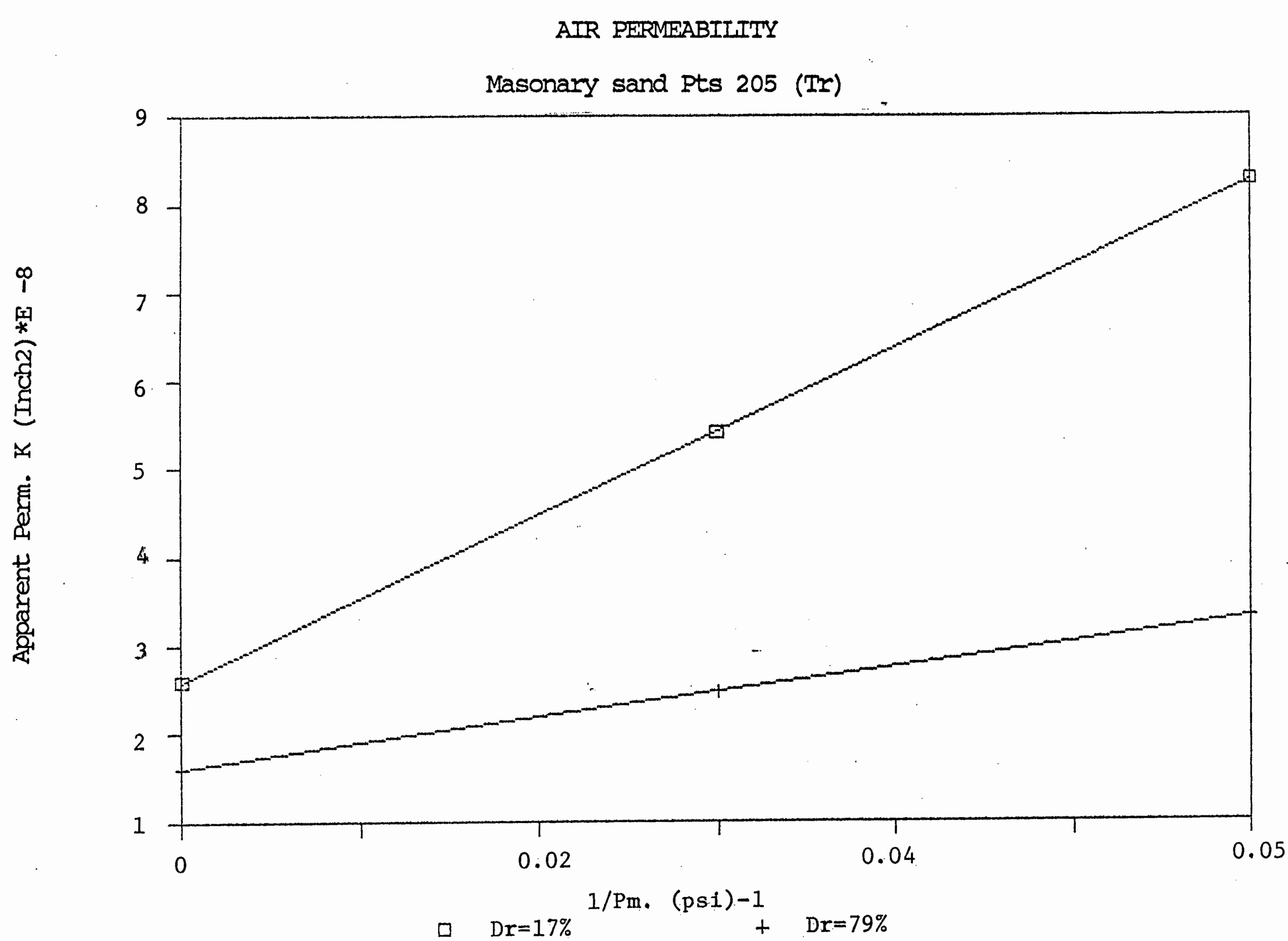
AIR PERMEABILITY
Masonary sand Pts 205 (Tr)
Apparent Perm. K (Inch2)*E -8
9
8
7
6
5
4
3
2
1
0
0.02
0.04
0.05
1/Pm. (psi)-1
Dr=17%
Dr=79%

Figure 26

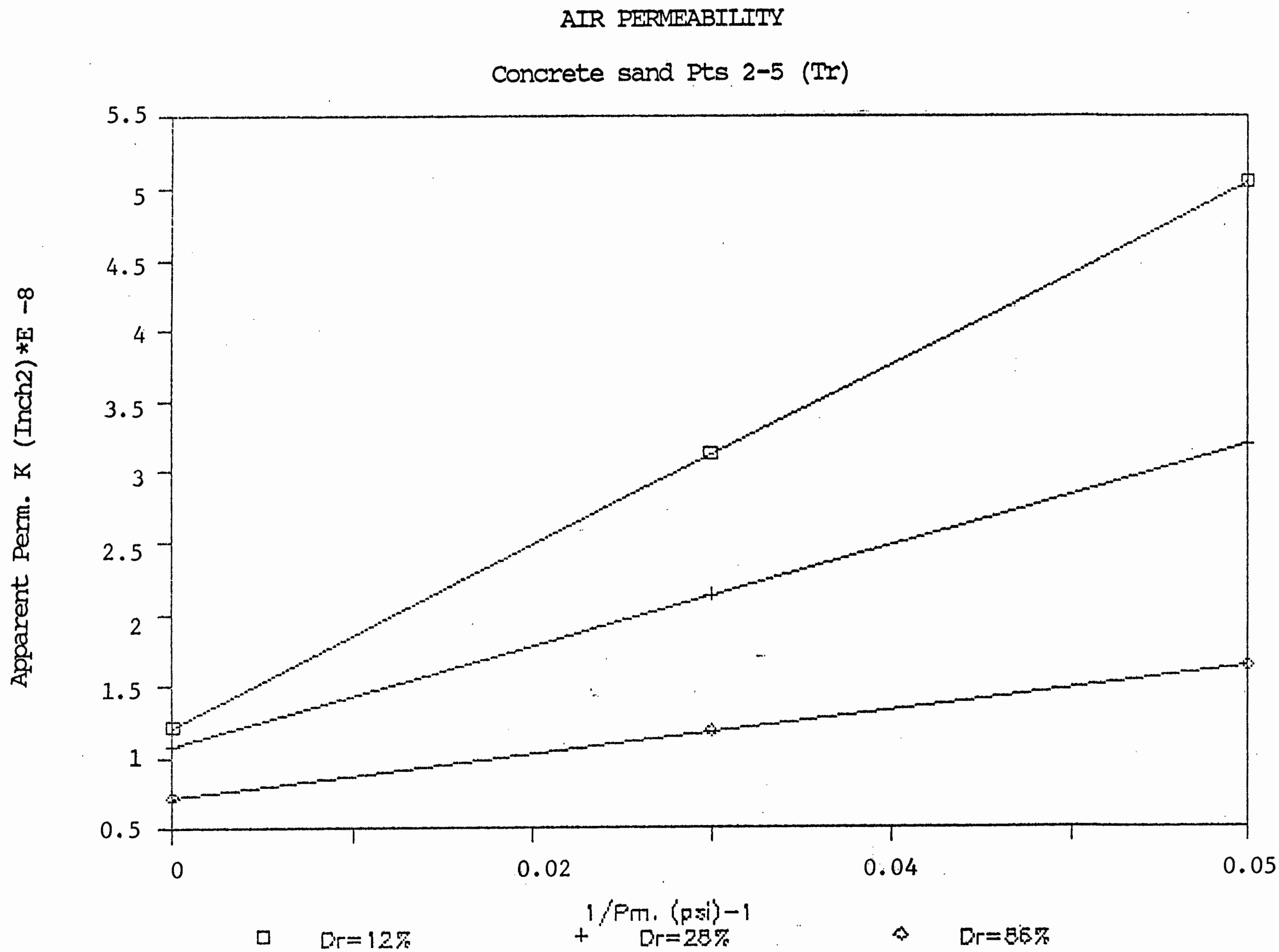
AIR PERMEABILITY
Concrete sand Pts 2-5 (Tr)
Apparent Perm. K (Inch2)*E -8
5.5
5
4.5
4
3.5
3
2.5
2
1.5
1
0.5
0
0.02
0.04
0.05
1/Pm. (psi)-1
Dr=12%
Dr=28%
Dr=86%

Figure 27

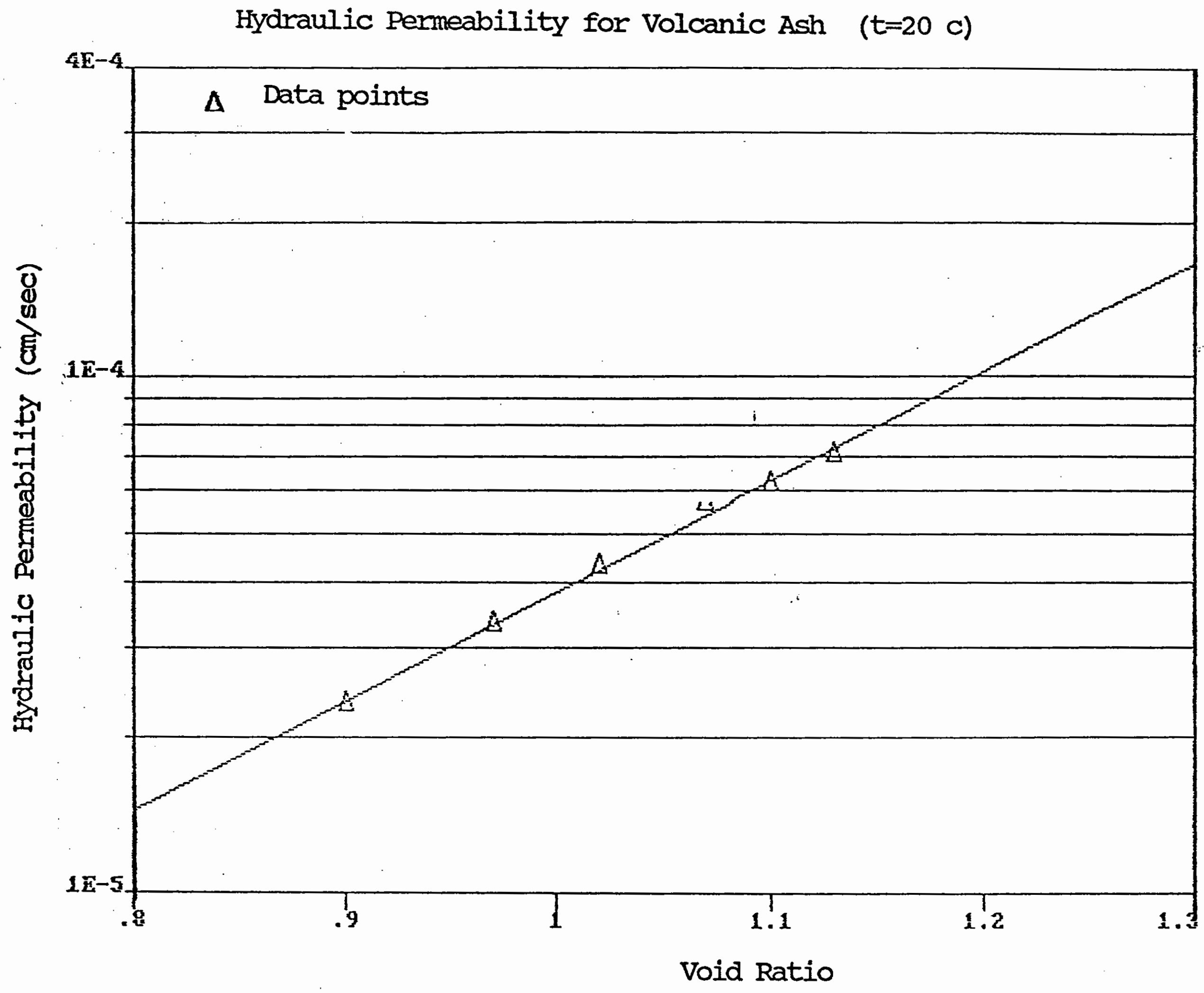
Hydraulic Permeability for Volcanic Ash (t=20 c)
Data points
4E-4
1E-4
1E-5
Hydraulic Permeability (cm/sec)
.8
.9
1
1.1
1.2
1.3
Void Ratio

Figure 28

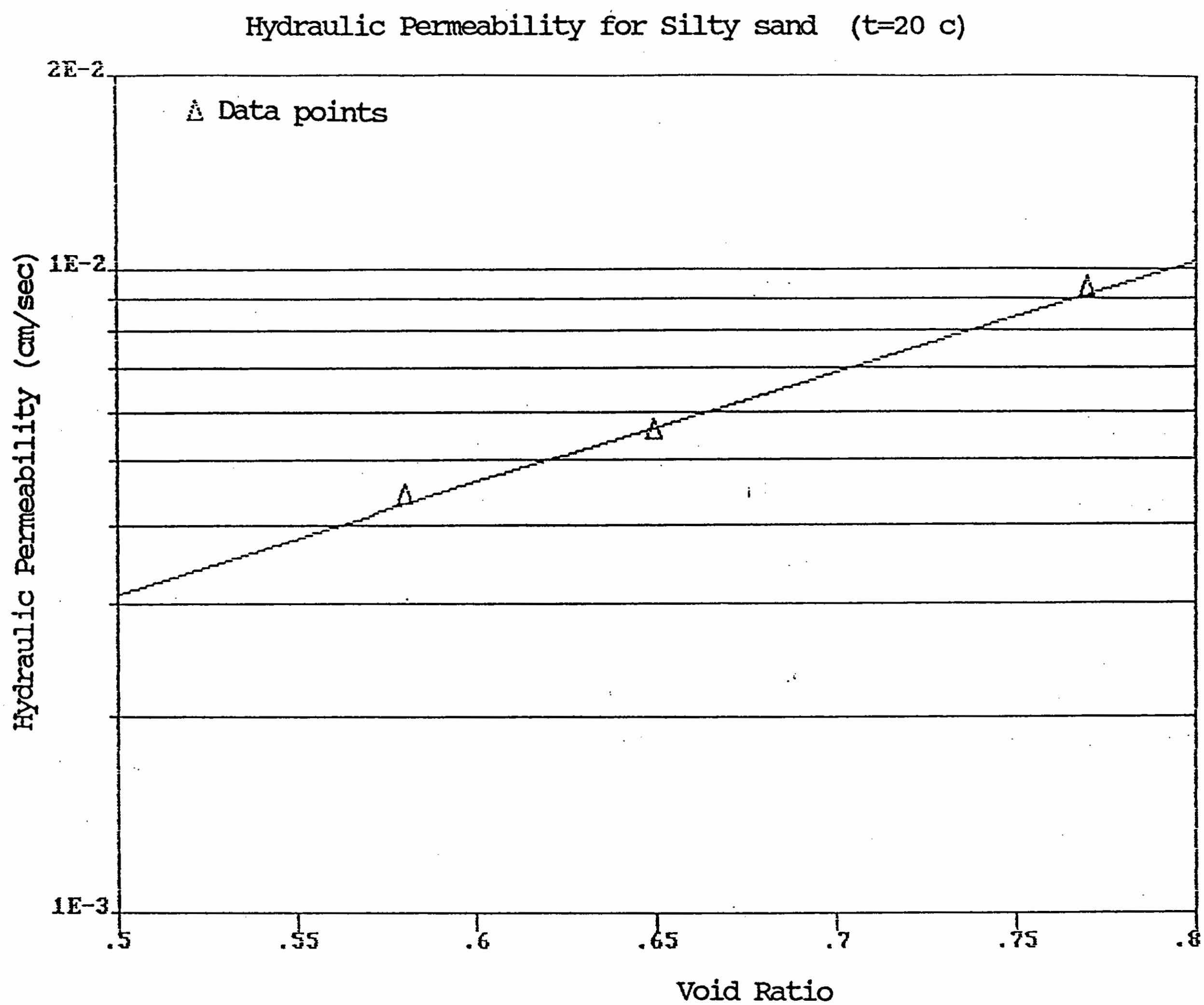
Hydraulic Permeability for Silty sand (t=20 c)
2E-2
1E-2
1E-3
Δ Data points
Hydraulic Permeability (cm/sec)
.5
.55
.6
.65
.7
.75
.8
Void Ratio

Figure 29

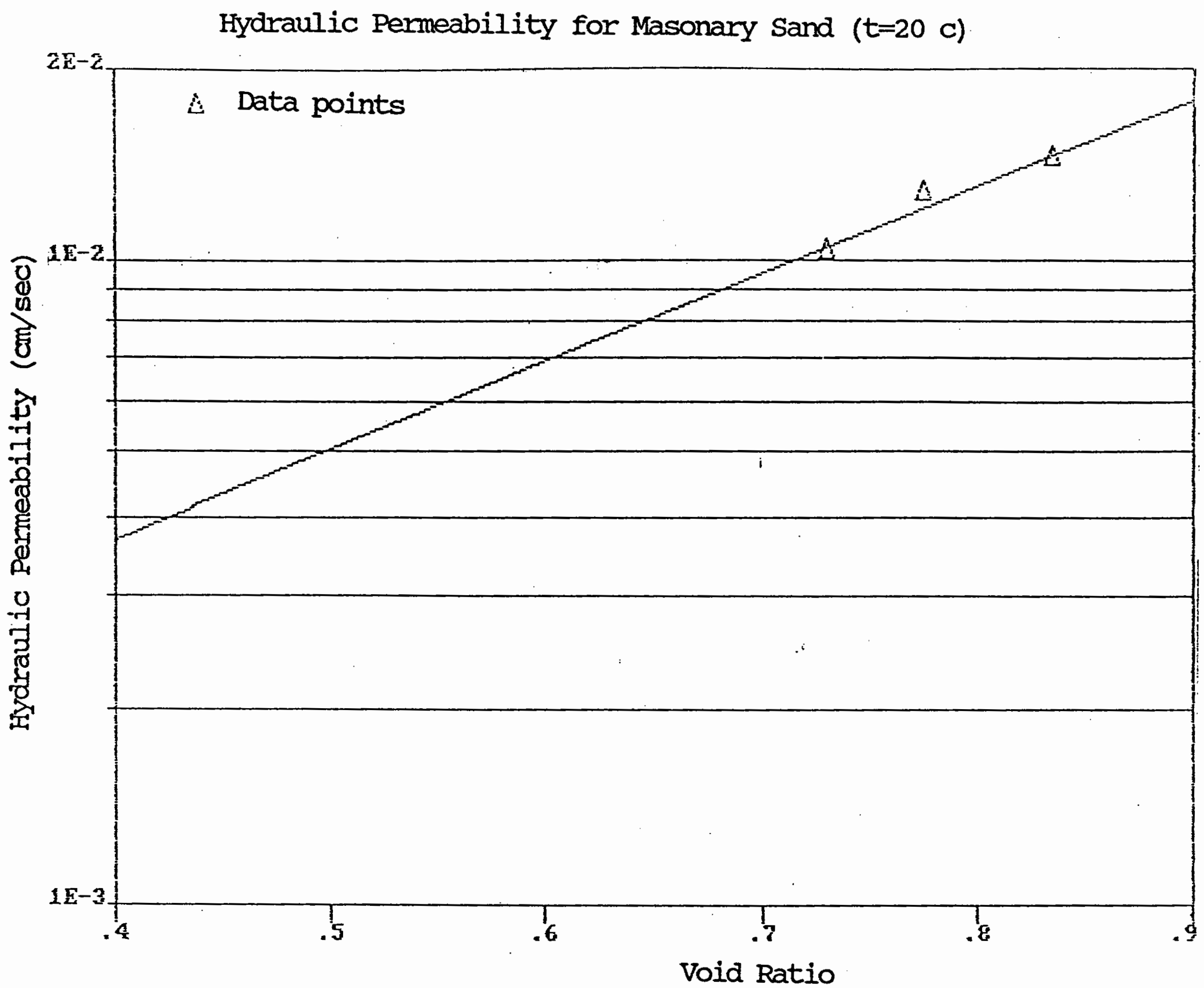

Hydraulic Permeability for Masonary Sand (t=20 c)
Data points
2E-2
1E-2
1E-3
Hydraulic Permeability (cm/sec)
.4
.5
.6
.7
.8
.9
Void Ratio

Figure 30

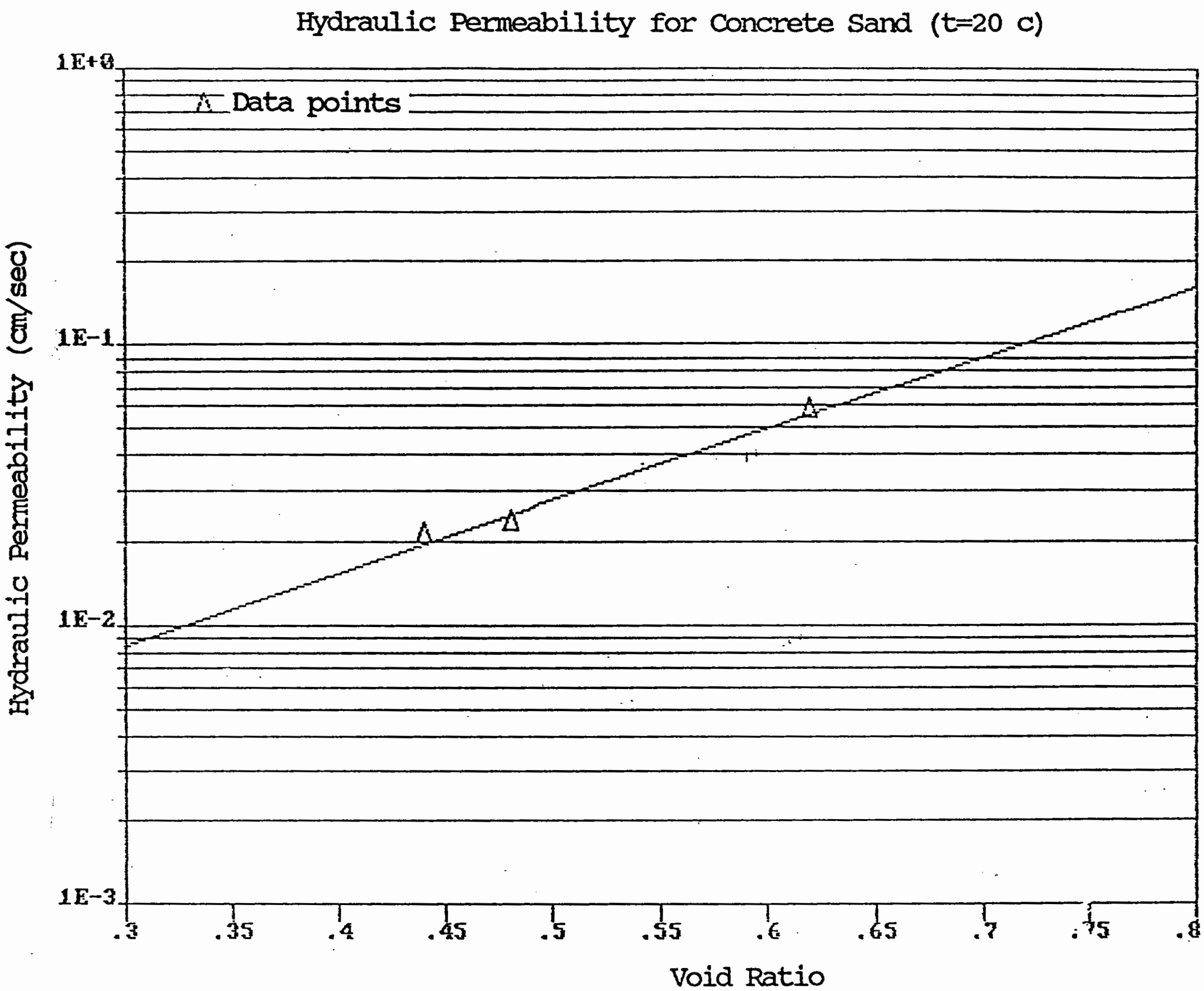
Hydraulic Permeability for Concrete Sand (t=20 c)
Data points
1E+0
1E-1
1E-2
1E-3
Hydraulic Permeability (cm/sec)
.3
.35
.4
.45
.5
.55
.6
.65
.7
.75
.8
Void Ratio

Figure 31

Discussion

From the results, it is clear that the hydraulic permeability coefficients obtained using Klinkenberg theory are close to the hydraulic permeability coefficients obtained using flow of water except for Ottawa sand where the laminar flow regime breaks down due to high flow rates (Reynolds number is greater than 10). For the same reason, the ratio between both permeabilities is closer to one for low permeable soil (laminar flow exists and Reynolds number less than 10) and different for high permeable soil (laminar flow starts breaking down) [see Table 1].

One of the interesting things noticed from the results is that the intrinsic permeability coefficient "K_S" increases as the void ratio increases for the same soil which shows the effect of the density of the soil on the permeability coefficient. The permeability reduces with increasing relative density of the soil. Also the value of the fitted line slope "b" increases as the void ratio "e" increases for the same soil.

The ratio between the hydraulic permeability obtained by Klinkenberg method and the hydraulic permeability by falling head method increases as the void ratio increases for the same soil. This ratio is greater than one for all the tested soils except for the concrete sand and the Ottawa sand "high permeable soils".

As noted before, measuring the permeability using water requires certain precautions since any air dissolved in the water tends to come out of solution and block some of the porous passages within the soil, yielding a value of the coefficient of permeability from the experimental results that is too low. Add for the above mentioned reason that the 100%

saturation required for permeability using water measurement is difficult to obtain. That leads us to conclude that the permeability coefficient obtained using air may be closer to the true permeability.

Several years ago FHWA sponsored a project to determine the permeability of soil in place. The results of this work were not completely satisfactory in that the techniques presented could not test the full range of permeabilities for soils included in pavement foundations. As we mention before, it is very difficult to measure low permeabilities in the field using water. This research shows that measuring the permeability to air and converting it to the value with water will work well with low permeability soils.

*Application of the New Technique on Connecticut's soil:

Typical soils for the state of Connecticut were tested in a previous research program (Long et al., 1987). These soils are typical of those found in Connecticut. As mentioned before, for high permeable soil laminar flow breakers down and the new technique mention will not be applicable. Hence, it was important to investigate the applicability of the new technique on typical soils for Connecticut. Table 2 shows the Reynold's Number of all the soils which had been tested on "the Conversion to the Unified Soil Classification System" research. It is clear from Table 2 that the Reynold's Numbers for all the soils tested are less than 10, indicating that laminar flow can be expected when testing with permeability and the new technique may be applied on most State of Connecticut soils. It should be mentioned that the Reynold's Number in Table 2 was computed using the highest flow rate use in our experiments and assuming the void ratio is about 0.5.

Conclusions

It has been the purpose of this research to investigate the relationship between permeability coefficients for soil using both liquid and gas. In particular attention has been directed to the flow of air through dry granular soils. Some conclusions that emerge from this research are as follows:

1. Darcy's law can be applied for gases flow through soil with some account of both compressibility and gas-slip.
2. Soil permeability coefficients obtained using liquids and gas will differ considerably, due to the phenomenon of gas slippage.
3. Air permeability of the soil is a linear function of reciprocal mean pressure.
4. Air permeability does not depend on the pressure difference as long as the mean pressure is constant.
5. At infinite pressure $(1/P_m) = 0$ the intrinsic permeability obtained using air flow will approach the intrinsic permeability obtained using water.
6. Both air permeability and water permeability coefficients increase with decreasing relative density of soil.
7. A new and better method for measuring the true permeability of granular soil is introduced by measuring the permeability using air flow and then converting it to the true one. This method overcomes the inaccuracy of measuring soil permeability with water due to the dissolved gases in water.

8. The above mentioned technique will work well for low permeable materials but has some limition for high permeable materials since the laminar flow regime breaks down for sufficiently high flow rates (at Reynolds number greater than 10).

9. The value of the true intrinsic permeability increases as the void ratio increases.

10. The value of the fitted line slope "b" increases as the void ratio increases for each type of soil.

11. The ratio between the true intrinsic permeability obtained using air and the one obtained using water increases as the void ratio increases. This ratio is greater than one for all the tested soils, exept for concrete
sand and Ottawa sand since the laminar flow regimes breaks down for high flow rates.

12. Finally, it is recommended that more research should be done on partially saturated granular soil and clay to verify the above mentioned technique. Also field experiments are needed to investigate the dimensionality effect.

Reynold's Number of Soil Samples on the U.S.C.S. Report

Soil Type	D_{10}(mm)	Modified R_n*
Brown Till	0.075	4.80
Brown silty sand	0.070	4.50
Light gray clay	0.001	0.064
Reddish, Brown line sand	0.053	3.4
Gray silty clay	0.0058	0.37
Silty sand	0.080	5.11
Reddish silty Gravelly sand	0.023	1.50
Reddish brown clay	0.001	0.064
Gray clay	0.001	0.064
Gray clay-silt	0.001	0.064
Red fine sand & silt	0.02	1.30

* Assuming e = 0.5

Table 2

REFERENCES

"ASTM Standard Test Method for Permeability of Rocks by Flowing Air", D4525-85, ASTM Standards, November 1985.

Bamforth, P.B. "The Relationship Between Permeability Coefficients for Concrete Obtained Using Liquid and Gas". Magazine of Concrete Research, Vol. 39, No. 138, March 1987.

Blight, G.E. "Flow of Air Through Soils", Journal of The Soil Mechanics and Foundation Division, ASCE, Vol. 97, No. SM4, April 1971.

Collins, R.E. "Flow of Fluids Through Porous Materials", Reinhold, N.Y., 1961.

Dybbs, A. and Edwards, R.V. "A New Look at Porous Media Fluid Mechanics - Darcy to Turbulent", from Fundamentals of Transport Phenomena In Porous Media, edited by: Bear and Corapcioglu, Martinus Nijhoff Publishers, 1984.

Ergun, S. and Orning, A.A. ,Ind. Eng. Chem., Vol. No. 1179, 1949.

Fanche, G.H. and Lewis, J.A., Ind. Eng. Chem., Vol. 25, No. 1139, 1933.

"FHWA In Situ Determination of Permeability of Base and Subbase Courses Phase I", Report No. FHWA-RD-78-21, December 1977.

Klinkenberg, L.J. The Permeability of Porous Media to Liquid and Gases, American Petrolum Institute Drilling and Production Practice, 1941.

Kundt, A. and Warburg, E. Poggendorf Ann. Physik., 155, 337, and 525, 1875.

Long, R.P., Demars, K.R., Covo, A., Mankbadi, R.R., Mekagaroon, V. and Shaheen, W., "Conversion to The Unified Soil Classification System", Final Report, Civil Engineering Department, The University of Connecticut, December 1987.

Matyas, E.L. "Air and Water Permeability of Compacted Soils", Permeability and Capillanity of soils, ASTM STP 417, P. 160, 1967.

Moore, C.A. and Alzayadi A. "Therotical Considerations of Movements of Gases Around Sanitary Land Fills", Report to U.S. EPA, 1975.

Rad, N.S. and Tumay, M.T. "Factors Affecting Sand Specimen Preparation by Raining", Geotechnical Testing Journal, GTJODJ, Vol. 10, No. 1, pp. 31-37, March 1987.

APPENDIX

Trapezoidal average.

Soil sample: Medium Conc. Snd Date: 06/26/87

Ws= 4.690 Pounds Length= 12.000 Inch.

AREA= 4.870 Inch sq. u air= 2.65E-9

Lt= 15.313 Inch. Pts 2-5 Dr= 28.000 %

mm Entr. Pi	(Hg)		mm Exit Pe	(Hg)	
1463.000	28.041	42.741	315.000	6.038	20.738
1302.000	24.955	39.655	265.000	5.079	19.779
1153.000	22.100	36.800	227.000	4.351	19.051
1016.000	19.474	34.174	192.000	3.680	18.380
871.000	16.694	31.394	157.000	3.009	17.709
731.000	14.011	28.711	125.000	2.396	17.096
588.000	11.270	25.970	95.000	1.821	16.521
448.000	8.587	23.287	67.000	1.284	15.984
307.000	5.884	20.584	45.000	0.863	15.563
170.000	3.258	17.958	25.000	0.479	15.179
0.000	0.000	14.700	0.000	0.000	14.700
0.000	0.000	14.700	0.000	0.000	14.700
0.000	0.000	14.700	0.000	0.000	14.700
0.000	0.000	14.700	0.000	0.000	14.700
0.000	0.000	14.700	0.000	0.000	14.700
0.000	0.000	14.700	0.000	0.000	14.700
0.000	0.000	14.700	0.000	0.000	14.700
0.000	0.000	14.700	0.000	0.000	14.700
0.000			0.000		
0.000			0.000		

mm Ps	(Wt)		Flow (Q)	Reading	1/Pm	*E+8 K (IN2)
345.000	0.489	15.189	153.000	100.000	0.030	2.080
285.000	0.404	15.104	137.810	90.000	0.032	2.212
230.000	0.326	15.026	121.540	80.000	0.035	2.320
188.000	0.266	14.966	105.880	70.000	0.037	2.410
150.000	0.212	14.912	88.480	60.000	0.040	2.489
123.000	0.174	14.874	72.210	50.000	0.042	2.550
100.000	0.142	14.842	57.460	40.000	0.046	2.716
85.000	0.120	14.820	42.710	30.000	0.050	2.838
74.000	0.105	14.805	28.400	20.000	0.055	2.996
70.000	0.099	14.799	15.260	10.000	0.060	3.183
0.000	0.000	14.700	0.000		0.000	0.000
0.000	0.000	14.700	0.000		0.000	0.000
0.000	0.000	14.700	0.000		0.000	0.000
0.000	0.000	14.700	0.000		0.000	0.000
0.000	0.000	14.700	0.000		0.000	0.000
0.000	0.000	14.700	0.000		0.000	0.000
0.000	0.000	14.700	0.000		0.000	0.000
0.000	0.000	14.700	0.000		0.000	0.000

0.000
0.000 0.000

Pi-Ps	Q/A	dp/Lt
27.553	31.417	1.799
24.552	28.298	1.603
21.774	24.957	1.422
19.207	21.741	1.254
16.482	18.168	1.076
13.837	14.828	0.904
11.129	11.799	0.727
8.466	8.770	0.553

****************** STRAIGHT LINE ******************
***************** MINIMUM SQUARE FIT **************

****
n= 10.000

	X	Y	XY	X^2
1.000	0.030	2.080	0.063	0.001
2.000	0.032	2.212	0.072	0.001
3.000	0.035	2.320	0.080	0.001
4.000	0.037	2.410	0.089	0.001
5.000	0.040	2.489	0.098	0.002
6.000	0.042	2.550	0.108	0.002
7.000	0.046	2.716	0.125	0.002
8.000	0.050	2.838	0.142	0.003
9.000	0.055	2.996	0.164	0.003
10.000	0.060	3.183	0.191	0.004
11.000	0.000	0.000	0.000	0.000
12.000	0.000	0.000	0.000	0.000
13.000	0.000	0.000	0.000	0.000
14.000	0.000	0.000	0.000	0.000
15.000	0.000	0.000	0.000	0.000
16.000	0.000	0.000	0.000	0.000
17.000	0.000	0.000	0.000	0.000
18.000	0.000	0.000	0.000	0.000
19.000	0.000	0.000	0.000	0.000
20.000	0.000	0.000	0.000	0.000

```
*****************************************************************
  sum(X)=   0.427      a=       35.289
  sum(Y)=  25.793      b=        1.074
 sum(XY)=   1.132
sum(X^2)=   0.019

   2.138
   2.215
   2.292
   2.372
   2.469
   2.564
   2.700
   2.843
   3.008
   3.191
   1.074
```